

Generalization of the simplicial depth: no vanishment outside the convex hull of the distribution support

Giacomo Francisci^{1,2}, Alicia Nieto-Reyes², and Claudio Agostinelli¹

¹University of Trento

²University of Cantabria

March 17, 2022

Abstract

The simplicial depth, like other relevant multivariate statistical data depth functions, vanishes right outside the convex hull of the support of the distribution with respect to which the depth is computed. This is problematic when it is required to differentiate among points outside the convex hull of the distribution support, with respect to which the depth is computed, based on their depth values. We provide the first two proposals to overcome this issue as well as several corresponding estimators, which do not vanish right outside the convex hull of the data. The properties of the proposals and of the corresponding estimators are studied, theoretically and by means of Monte Carlo simulations. Furthermore, the proposed methodology can be generally applied and it is here extended to the other most well-know instance of depth: the halfspace, or Tukey, depth, which suffers from the same problematic.

Keywords: Classification, Consistency, Empirical depth, Halfspace depth, Multivariate statistical data depth, Multivariate symmetry, Vanishment outside the convex hull.

1 Introduction

Multivariate statistical data depth functions provide an order of the elements of a space on \mathbb{R}^p , $p \geq 1$, with respect to a probability distribution on the space. Regina Liu [1990] introduced the simplicial depth as an instance of depth that satisfies some good theoretical properties that later became the constituting properties of the notion of statistical data depth [Zuo and Serfling, 2000a]. Since then, the simplicial depth has been broadly studied and applied in the literature; see, for instance, Arcones and Giné [1993], Arcones et al. [1994], Li et al. [2012]. A particularity of the simplicial depth is that it provides zero depth value to

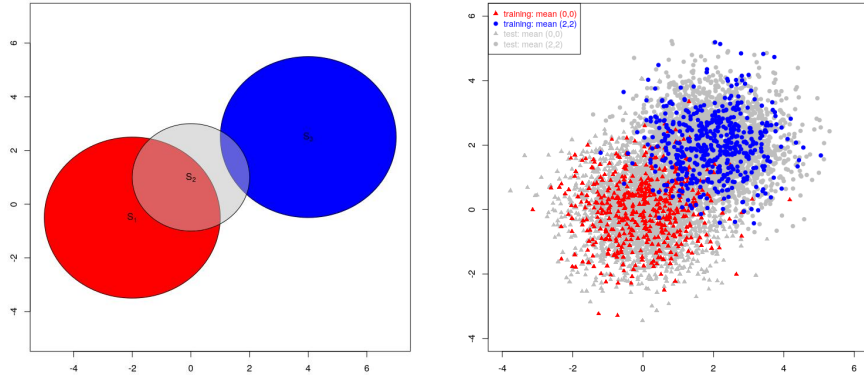


Figure 1: Left plot: Example of of three compact supports where the set $S_2 \setminus (S_1 \cup S_3)$ is non-empty. Right plot: 3000 random draws from each of two bivariate normal distributions: mean $(0, 0)$ as triangles and mean $(2, 2)$ as circles. The first 500 elements of each sample are depicted in color.

the elements of the space that are outside the convex hull of the distribution support with respect to which the depth is computed. Additionally, the sample simplicial depth gives value zero to every point in the space outside the convex hull of the sample. Our main aim is to address these two aspects as they become problematic for those applications in which it is required to discriminate among different elements of the space.

Let us first focus on the theoretical case of not being able to differentiate among elements outside the convex hull of a distribution support, which is problematic, for example, on applications found in medicine such as neurodegenerative diseases. For instance, let $P^{(i)}$, $i = 1, 2, 3$, be three multivariate distribution functions and let us denote by S_i , $i = 1, 2, 3$, the convex hulls of the corresponding supports. Suppose we aim to divide S_2 into two groups: the points that are deeper in $P^{(1)}$ than in $P^{(3)}$ and its complementary; while keeping the occurrence of ties to a minimum. If $S_2 \setminus (S_1 \cup S_3)$ is non-empty, as illustrated in the left plot of Figure 1 in \mathbb{R}^2 , the simplicial depth gives zero depth to each point in this set when computed with respect to either $P^{(1)}$ or $P^{(3)}$. This might be the case of a disease with different stages: $P^{(1)}$ refers to patients in the early stage of the disease, $P^{(3)}$ to patients in the last stage of the disease and $P^{(2)}$ to patients in an intermediate stage of the disease. In particular, we would aim to know which of the patients in the intermediate stage of the disease are in a stage more similar to the last stage of the disease than to the early, or viceversa.

The above scenario can be particularized to $P^{(2)}$ being a mixture of two distributions that result of incurring on an error on $P^{(1)}$ and on $P^{(3)}$ so that $S_2 \setminus (S_1 \cup S_3)$ is non-empty; the error on $P^{(1)}$ not being necessarily equivalent to

the one on $P^{(3)}$. If no error is incurred, we are in front of a theoretical supervised classification problem, where $S_2 \setminus (S_1 \cup S_3)$ is empty; and the vanishing outside the convex hull of the distribution support would not be problematic. However, if $P^{(1)}$ and $P^{(3)}$ are unknown, the depth is estimated through its sample version which suffers from the problem of vanishing outside the convex hull of the data sample. In general, a supervised classification problem consists of two samples $X = \{X_1, \dots, X_m\}$ and $Z = \{Z_1, \dots, Z_o\}$, drawn respectively from $P^{(1)}$ and $P^{(3)}$ and a third sample $Y = \{Y_1, \dots, Y_n\}$, where some of the elements of Y are drawn from $P^{(1)}$ and the others from $P^{(3)}$. The aim is to classify each element of Y as being drawn from either distribution $P^{(1)}$ or $P^{(3)}$. The X and Z are known as training samples and the Y as test sample. This is illustrated in the right plot of Figure 1 in \mathbb{R}^2 , where the X and Z are plotted respectively in red and blue and the Y in grey. In the particular setting of the plot, $P^{(1)}$ and $P^{(3)}$ are both normally distributed. It can be easily observed from the right plot of Figure 1 that there are elements of Y which are simultaneously outside both convex hulls, the one of X and the one of Z . If we were to classify the elements of Y using a supervised classification methodology based on statistical depth [see for example, Li et al., 2012], we would like the depth value of each Y_i , $i = 1, \dots, n$, with respect to the empirical distribution associated to X , to differ from the value obtained when computed with respect to the empirical distribution associated to Z . Making use of the sample simplicial depth, it is not possible to classify the elements of Y that are simultaneously outside the convex hull of X and Z because the sample simplicial depth of these points is zero when computed with respect to either the empirical distribution associated to X or Z .

We provide a methodology that generalizes the simplicial depth resulting in a depth function that does not vanish right outside the convex hull of the distribution support. The methodology is based on linear combinations of independent random variables. As multivariate symmetry [Zuo and Serfling, 2000b] is a key concept in the notion of depth, we dedicate Section 2 to study the conditions under which symmetry is inherited under affine combinations. This has far reaching implications as affine combinations are widely applied in statistics, for instance, in dimension reduction problems. Moreover, the non-symmetry of an affine combination will imply the non-symmetry of the original distribution, under certain assumptions. In Section 3, we introduce two different approaches to generalize the simplicial depth and provide different sample versions of them that do not vanish right outside the convex hull of the data sample. We study the consistency of these sample versions.

The methodology proposed can be extended to other instances of depth and we extend it in Section 4 to the halfspace depth [Tukey, 1975], as it is the other very well-known instance of depth for multivariate spaces and suffers from the same problematic than the simplicial depth; of taking zero value outside the convex hull of the distribution support and its sample version taking zero value outside the convex hull of the data. We study their theoretical properties, including consistency of the sample version. A first attempt to solve the problematic for the sample version of the Tukey depth was pursued in Einmahl et al.

[2015]. The proposal there has, however, several shortcomings: it requires of certain restrictive assumptions that do not include common distributions like the normal distribution, used in the right plot of Figure 1, or distributions with compact support such as the uniform distribution in left plot of Figure 1. Additionally, as stated there, their methodology is not applicable to other instances of depth like the simplicial depth. A second attempt to improve the sample Tukey depth is presented in the pre-print Nagy and Dvořák [2019]. However, as described there, the estimator requires large sample sizes with a resulting bivariate estimated depth value instead of scalar. Additionally, it needs restrictive conditions, such as elliptically symmetric distributions, for a reasonable behavior.

Section 5 contains the proofs of the results in previous sections and some further results. In Section 6 we present some Monte Carlo simulations where the two main contributions are studied empirically, for distributions with overlapping and non-overlapping convex-hulls. The first setting includes a missing data scenario. The second one is an innovative scenario in the statistical literature that is helpful for studying the closeness to some fixed groups of elements of other distinct group(s). For instance, the example of degenerative diseases provided above. Future work is commented in Section 7.

2 Symmetry of random variables

We prove under which notions of symmetry the affine combinations of independent and symmetric random variables are symmetric. The most well-known notions of symmetry in the literature are spherical, elliptical, central, angular and halfspace symmetry, where each is a generalization of the previous one. According to Serfling [2004], a random vector $X \in \mathbb{R}^p$ is *spherically symmetric* about a point $\mu \in \mathbb{R}^p$ if $X - \mu$ and $U(X - \mu)$ are identically distributed for any orthonormal matrix U . Different definitions of elliptical symmetry are possible. We choose the weak version in Ley and Paindaveine [2011]: a random vector X in \mathbb{R}^p is *elliptically symmetric* about a point $\mu \in \mathbb{R}^p$ if there exists a nonsingular matrix V such that VX is spherically symmetric about $V\mu$. According to Serfling [2004], a random vector X in \mathbb{R}^p is *centrally symmetric* about a point $\mu \in \mathbb{R}^p$ if $X - \mu$ and $\mu - X$ are identically distributed. Note that the notions of spherical, elliptical and central symmetry coincide for univariate random variables. The notion of angular symmetry was introduced in Liu [1990]: a random vector X in \mathbb{R}^p is *angularly symmetric* about a point $\mu \in \mathbb{R}^p$ if $(X - \mu) / \|X - \mu\|$ and $(\mu - X) / \|X - \mu\|$ are identically distributed. This was generalized in Zuo and Serfling [2000b] by defining a random vector X in \mathbb{R}^p to be *halfspace symmetric* about μ if $\mathbb{P}(X \in H) \geq \frac{1}{2}$ for every closed halfspace H with μ on the boundary.

The next proposition states that all these notions of symmetry are preserved under affine transformations.

Proposition 1 *Let X be a random variable on \mathbb{R}^p that is symmetric about $\mu \in \mathbb{R}^p$ with respect to either spherical, elliptical, central, angular or halfspace*

symmetry. Then, for any $\lambda \in \mathbb{R}$ and $b \in \mathbb{R}^p$, $\lambda X + b$ is symmetric about $\lambda\mu + b$ with respect to the same notion of symmetry.

If a distribution is spherically, elliptically or centrally symmetric, the center of symmetry is unique. If the distribution is angular or halfspace symmetric, the center is unique but for the degenerate case in which the distribution on \mathbb{R}^p , $p > 1$, has all its probability mass on a line with more than one median [Zuo and Serfling, 2000b, Theorem 2.1, Lemma 2.3]. Note that, when the center of symmetry is not unique, Proposition 1 remains valid for each center of symmetry.

The next two results concern the inheritance under affine combinations of spherical, elliptical and central symmetry.

Proposition 2 *Let X_1, \dots, X_n be independent and identically distributed random variables on \mathbb{R}^p that are symmetric about $\mu \in \mathbb{R}^p$ with respect to either spherical, elliptical or central symmetry. For any $\lambda_1, \dots, \lambda_n \in \mathbb{R}$ and $b \in \mathbb{R}^p$ then $\sum_{i=1}^n \lambda_i X_i + b$ is symmetric about $\sum_{i=1}^n \lambda_i \mu + b$ with respect to the same notion of symmetry.*

The above proposition is generalized below to non-identically distributed random variables for the notions of spherical and central symmetry.

Proposition 3 *Let X_1, \dots, X_n be independent random variables on \mathbb{R}^p . For either spherical or central symmetry, let X_i be symmetric about $\mu_i \in \mathbb{R}^p$ for all $i = 1, \dots, n$. For any $\lambda_1, \dots, \lambda_n \in \mathbb{R}$ and $b \in \mathbb{R}^p$ then $\sum_{i=1}^n \lambda_i X_i + b$ is symmetric about $\sum_{i=1}^n \lambda_i \mu_i + b$ with respect to the same notion of symmetry.*

For elliptically symmetric non-identically distributed random variables, we have the following corollary of Proposition 3.

Corollary 4 *Let X_1, \dots, X_n be as in Proposition 3, but with X_i elliptically symmetric about $\mu_i \in \mathbb{R}^p$ for each $i = 1, \dots, n$. Then, $\sum_{i=1}^n \lambda_i X_i + b$ is centrally symmetric about $\sum_{i=1}^n \lambda_i \mu_i + b$ for any $\lambda_1, \dots, \lambda_n \in \mathbb{R}$ and $b \in \mathbb{R}^p$.*

For a series of counterexamples on angular and halfspace symmetry related to the above results, see the supplementary material, Section A.

3 Generalization of the simplicial depth

The simplicial depth [Liu, 1990] of a point $x \in \mathbb{R}^p$ with respect to a distribution P on \mathbb{R}^p is $d(x; P) := \int \mathbf{I}(x \in \Delta[x_1, \dots, x_{p+1}]) dP(x_1) \cdots dP(x_{p+1})$, with $\Delta[x_1, \dots, x_{p+1}]$ denoting the closed simplex with vertices on x_1, \dots, x_{p+1} and \mathbf{I} the indicator function. The objective of this section is to modify the simplicial depth in a manner that the depth value of the points in \mathbb{R}^p that are outside the convex hull of the support of P is not necessarily zero. We pursue it in two different manners: Definition 5 uses an enlargement of the simplex and Definition 7 computes the simplicial depth with respect to a transformation of the original distribution with respect to which the depth is evaluated. This transformation is introduced below in Definition 6.

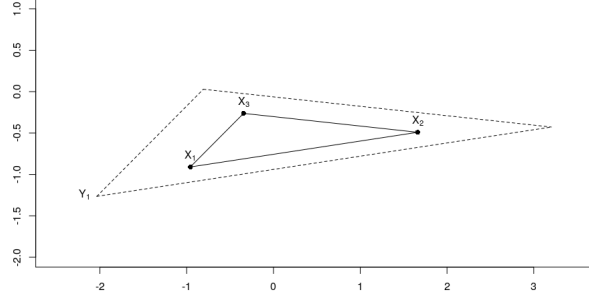


Figure 2: Simplex generated by the random draws of three independent standard normal distribution in \mathbb{R}^2 , X_1 , X_2 and X_3 (solid line), and the enlarged simplex for $\sigma = 2$ (dash line), which has $Y_1 := 2X_1 - 1/3 \sum_{j=1}^3 X_j$ as a vertex.

Definition 5 Given $\sigma > 1$, the simplex enlarged σ -simplicial depth of a point $x \in \mathbb{R}^p$ with respect to a distribution P on \mathbb{R}^p is

$$d_{\Delta}(x; P) := \int \mathbf{I}(x \in \Delta_{\sigma}[x_1, \dots, x_{p+1}]) dP(x_1) \cdots dP(x_{p+1}),$$

where $\Delta_{\sigma}[x_1, \dots, x_{p+1}] := \Delta[y_1, \dots, y_{p+1}]$ with $y_i = \sigma x_i + (1-\sigma)/(p+1) \sum_{j=1}^{p+1} x_j$ for $i = 1, \dots, p+1$.

We illustrate Definition 5 in Figure 2, where it is shown a simplex in \mathbb{R}^2 and the corresponding enlarged simplex for $\sigma = 2$. If we allow σ to take value 1 in the definition, there is no enlargement of the simplex and we are left with the simplicial depth. Furthermore, the case $0 < \sigma < 1$ corresponds to a reduction of the simplex, whereas for $\sigma = 0$ the simplex degenerates into its centroid. The results presented in this paper are valid for $\sigma > 0$. We state $\sigma > 1$, though, because our interest lies in this subset.

Definition 6 Given P a distribution on \mathbb{R}^p and $\sigma > 1$, the σ -transformation of P , P_{σ} , is the distribution of the random variable $\sigma X_1 + (1-\sigma)/(p+1) \sum_{j=1}^{p+1} X_j$, where X_1, \dots, X_{p+1} are independent and identically distributed random variables with distribution P .

To illustrate the σ -transformation of P , Figure 2 contains the realizations of three independent random variables with the standard normal distribution in \mathbb{R}^2 , X_1, X_2 and X_3 , and the random variable $\sigma X_1 + (1-\sigma)/3 \sum_{j=1}^3 X_j$, with $\sigma = 2$, which is denoted by Y_1 in the plot. If we allow σ to be 1 in the definition, no transformation is performed on P , while for $0 \leq \sigma < 1$ is equivalent to the one mentioned above.

Definition 7 Given $\sigma > 1$, the distribution enlarged σ -simplicial depth of a point $x \in \mathbb{R}^p$ with respect to a distribution P on \mathbb{R}^p is

$$d_\sigma(x; P) := \int \mathbf{I}(x \in \Delta[x_1, \dots, x_{p+1}]) dP_\sigma(x_1) \cdots dP_\sigma(x_{p+1}).$$

Note that $d_\sigma(x; P)$ is the simplicial depth of x with respect to P_σ .

Remark 8 The simplex enlarged σ -simplicial depth is a refinement of the simplicial depth that makes use of dependent vertices in the simplex while the distribution enlarged σ -simplicial depth benefits from independent vertices in the simplex. This is easily observed by realizing that

$$\begin{aligned} d_\Delta(x; P) &= \int \mathbf{I}(x \in \Delta[l(x_1, \dots, x_{p+1})]) dP(x_1) \cdots dP(x_{p+1}) \text{ and} \\ d_\sigma(x; P) &= \int \mathbf{I}(x \in \Delta[s(x_1, \dots, x_{(p+1)^2})]) dP(x_1) \cdots dP(x_{(p+1)^2}), \end{aligned}$$

with

$$\begin{aligned} l(x_1, \dots, x_{p+1}) &:= (\sigma x_1 + \frac{1-\sigma}{p+1} \sum_{j=1}^{p+1} x_j, \dots, \sigma x_{p+1} + \frac{1-\sigma}{p+1} \sum_{j=1}^{p+1} x_j) \text{ and} \\ s(x_1, \dots, x_{(p+1)^2}) &:= (\sigma x_1 + \frac{1-\sigma}{p+1} \sum_{j=1}^{p+1} x_j, \dots, \sigma x_{1+p^2+p} + \frac{1-\sigma}{p+1} \sum_{j=1+p^2+p}^{(p+1)^2} x_j). \end{aligned}$$

Before studying the theoretical properties of the two definitions of the σ -simplicial depth, we examine in the next subsection the transfer of regularity conditions from P to P_σ .

3.1 Properties of P_σ

We first recall that a distribution P is *smooth* if $P(L) = 0$ for any hyperplane $L \subset \mathbb{R}^p$ [Massé, 2004, Condition (S)].

Theorem 9 Let P be a distribution on \mathbb{R}^p and $\sigma > 1$. If P is a continuous distribution (or respectively absolutely continuous or smooth), the σ -transformation of P , P_σ , is a continuous distribution (or respectively absolutely continuous or smooth).

The following result concerns the transfer of symmetry from P to P_σ .

Theorem 10 Let P be a distribution on \mathbb{R}^p and $\sigma > 1$. If P is either spherical, elliptical or centrally symmetric about $\mu \in \mathbb{R}^p$, then P_σ is symmetric about μ with respect to the same notion of symmetry.

The next two results are useful in computing the first and second order moments of P_σ given P .

Proposition 11 *Let X be a random variable with distribution P on \mathbb{R}^p . If P is centrally symmetric about a point $\mu \in \mathbb{R}^p$ and the expected value of X , $\mathbb{E}(X)$, exists, then $\mathbb{E}(X) = \mu$.*

Note that the normal distribution satisfies the hypothesis of Proposition 11.

Proposition 12 *Let $\sigma > 1$, X_1, \dots, X_{p+1} be independent and identically distributed random variables with distribution P on \mathbb{R}^p , $\lambda_1 := \sigma + (1 - \sigma)(p + 1)$ and $\lambda_i := (1 - \sigma)(p + 1)$ for $i = 2, \dots, p + 1$. If the covariance matrix of X_1 , Σ , exists the covariance matrix of $\sum_{i=1}^{p+1} \lambda_i X_i$ is given by $\left(\sigma^2 + \frac{1 - \sigma^2}{p+1}\right) \Sigma$.*

A direct consequence, of the above results is the following example.

Example 13 *If P is normally distributed with mean μ and covariance matrix Σ , $P \sim \mathbf{N}(\mu, \Sigma)$, then for all $\sigma > 1$, $P_\sigma \sim \mathbf{N}\left(\mu, \left(\sigma^2 + \frac{1 - \sigma^2}{p+1}\right) \Sigma\right)$. Equivalently, for all $\tau > 1$, $P_{\sqrt{\left(1 + \frac{1}{p}\right)\tau^2 - \frac{1}{p}}} \sim \mathbf{N}\left(\mu, \tau^2 \Sigma\right)$.*

3.2 Properties of the σ -simplicial depth

We study the properties of the simplex and distribution enlarged σ -simplicial depths below. Proposition 14 examines them as a function of σ and Theorems 15 and 17 for a fixed σ .

Proposition 14 *The simplex enlarged σ -simplicial depth as a function of sigma is monotonically nondecreasing and continuous on the right. If computed with respect to a smooth distribution, the simplex and distribution enlarged σ -simplicial depths are continuous as a function of sigma. Moreover, the distribution enlarged σ -simplicial depth is monotonically nondecreasing when computed with respect to elliptical distributions.*

The above result ensures that for any smooth P , when σ gets close to 1, the σ -simplicial depths have a similar behavior to that of the simplicial depth. Additionally, these functions can only have jump discontinuities and, in particular, they can only have at most countably many of them. The below results show that the σ -simplicial depths satisfy properties put forward in defining the simplicial depth.

Theorem 15 *The simplex enlarged σ -simplicial depth is (i) affine invariant, (ii) vanishes at infinity and is (iii) upper semicontinuous as a function of x . Additionally, if computed with respect to a smooth distribution, it is also (iv) continuous as a function of x .*

The simplex enlarged σ -simplicial depth does not satisfy the maximality at the center property nor it is monotonically decreasing along rays from this point even for spherically symmetric distributions (see Section B of the Appendix for a counterexample). However, for $p = 1$ it is monotone for the points outside the convex hull of the support.

Proposition 16 *Let $\sigma > 1$, P a distribution function on \mathbb{R} and S the convex hull of the support of P . Then for any $x, y \in \mathbb{R} \setminus S$ with $|x| \geq |y|$, we have that $d_\Delta(x; P) \leq d_\Delta(y; P)$.*

Theorem 17 *The distribution enlarged σ -simplicial depth is (i) affine invariant, (ii) vanishes at infinity and is (iii) upper semicontinuous as a function of x . Additionally, if computed with respect to a smooth distribution, it is also (iv) continuous as a function of x . Furthermore, if computed with respect to a smooth distribution that is centrally symmetric about a point $\mu \in \mathbb{R}^p$, then the σ -simplicial depth satisfies the (v) maximality at the center property and is (vi) monotone nonincreasing along rays through the center.*

The simplicial depth satisfies (v) and (vi) for angularly symmetric distributions. It is not generally true that if P is angularly symmetric, then also P_σ is. However, Theorem 10 ensures that if P is centrally symmetric about μ , then P_σ is centrally symmetric about μ , which implies that P_σ is angularly symmetric.

Given a statistical data depth, d , with respect to a distribution P on \mathbb{R}^p and $\alpha \geq 0$, the associated depth trimmed region is $\{x \in \mathbb{R}^p : d(x; P) \geq \alpha\}$. According to Zuo and Serfling [2000c, Theorem 3.1], the depth trimmed regions associated to the simplicial depth satisfy a series of properties that we elaborate below for the σ -simplicial depths.

Theorem 18 *The depth trimmed regions based on the simplex and distribution enlarged σ -simplicial depth are (i) affine equivariant, (ii) nested and (iii) if P is smooth, compact. Moreover, for the distribution enlarged σ -simplicial depth, they are (iv) connected if P is smooth and centrally symmetric.*

Corollary 19 *If P is smooth, then there exists at least: (i) a μ_σ such that $d_\sigma(\mu_\sigma; P) = \sup_{x \in \mathbb{R}^p} d_\sigma(x; P)$ and (ii) a μ_Δ such that $d_\Delta(\mu_\Delta; P) = \sup_{x \in \mathbb{R}^p} d_\Delta(x; P)$.*

3.3 Definition and properties of the empirical σ -simplicial depth

A sample X_1, \dots, X_n of random draws from a distribution P gives rise to the empirical distribution P_n . We provide, in the following definitions, sample versions for the simplex enlarged (Definition 20) and the distribution enlarged (Definitions 21 and 23) σ -simplicial depth functions.

Definition 20 *Let P be a given distribution on \mathbb{R}^{p-1} , $\sigma > 1$, $n \geq p$ and P_n the empirical distribution associated to a sample X_1, \dots, X_n of random draws taken from P . For any $x \in \mathbb{R}^{p-1}$,*

$$d_{\Delta, n}(x; P) := \binom{n}{p}^{-1} \sum_{1 \leq i_1 < \dots < i_p \leq n} \mathbf{I}(x \in \Delta_\sigma[X_{i_1}, \dots, X_{i_p}]).$$

Definition 21 *Let P be a given distribution on \mathbb{R}^{p-1} , $\sigma > 1$, $n \geq p^2$ and P_n the empirical distribution associated to a sample X_1, \dots, X_n of random draws*

taken from P . Let $k := k(n, p)$ be the greatest integer less than or equal to n/p . Then, for any $x \in \mathbb{R}^{p-1}$,

$$d_{\sigma,k}(x; P) := \binom{k}{p}^{-1} \sum_{1 \leq i_1 < \dots < i_p \leq k} \mathbf{I}(x \in \Delta[Y_{i_1}, \dots, Y_{i_p}])$$

with $Y_i = \sigma X_{1+(i-1)p} + \frac{1-\sigma}{p} \sum_{j=1}^p X_{j+(i-1)p}$ for $i = 1, \dots, k$.

Remark 22 Note that Y_1, \dots, Y_k in Definition 21 are random draws from P_σ each obtained as linear combinations of p random draws from P . Thus, $d_{\sigma,k}(\cdot; P) = d_k(\cdot, P_\sigma)$, with $d_k(\cdot, P_\sigma)$ denoting the sample simplicial depth based on k random draws from the distribution P_σ . Taking $\sigma = 1$, we obtain $d_{\sigma,k}(\cdot; P) = d_k(\cdot, P)$, retrieving the sample simplicial depth, but based only on k of the n random draws X_1, \dots, X_n .

The sample σ -simplicial depth of Definition 21 is a computationally efficient estimator of the distribution enlarged σ -simplicial depth, which makes it ideal in the large sample size scenario, for instance in big data analysis. For small sample sizes we recommend to make use of the full sample X_1, \dots, X_n and, thus, we propose the alternative definition below. For further insight on it, see the Appendix, Section C.

Definition 23 Let P be a given distribution on \mathbb{R}^{p-1} , $\sigma > 1$, $n \geq p^2$ and P_n the empirical distribution associated to a sample X_1, \dots, X_n of random draws taken from P . Then, for any $x \in \mathbb{R}^{p-1}$,

$$d_{\sigma,n}(x; P) := \frac{(n-p^2)!}{n!} \sum_A \mathbf{I}(x \in \Delta[Y_{i_1, j_{1,1}, \dots, j_{1,p-1}}, \dots, Y_{i_p, j_{p,1}, \dots, j_{p,p-1}}]),$$

where $A := \{i_1, \dots, i_p, j_{1,1}, \dots, j_{p,p-1} \in \{1, \dots, n\} : \text{all indexes differ}\}$ and $Y_{i_k, j_{k,1}, \dots, j_{k,p-1}} := \left(\sigma + \frac{1-\sigma}{p}\right) X_{i_k} + \frac{1-\sigma}{p} \sum_{l=1}^{p-1} X_{j_{k,l}}$ for $k = 1, \dots, p$.

Taking $\sigma = 1$ in $d_{\sigma,n}(\cdot; P)$, we retrieve the ranking provided by the empirical simplicial depth.

The next results study the properties of these estimators.

Proposition 24 For any distribution P on \mathbb{R}^p and any $x \in \mathbb{R}^p$, the function

$$\begin{aligned} [1, \infty) &\rightarrow [0, 1] \\ \sigma &\mapsto d_{\Delta,n}(x; P) \end{aligned}$$

is monotonically nondecreasing for each realization of the random variables X_1, \dots, X_n , drawn with distribution P .

The above result is not valid in general for either of the estimators of the distribution enlarged σ -simplicial depth.

Proposition 25 For any distribution P on \mathbb{R}^p , $d_{\Delta,n}(\cdot; P)$ is a U -statistic for the estimation of $d_{\Delta}(\cdot; P)$ while $d_{\sigma,k}(\cdot; P)$ and $d_{\sigma,n}(\cdot; P)$ are U -statistics for the estimation of $d_{\sigma}(\cdot; P)$.

Thanks to Proposition 25, the theoretical results for the empirical σ -simplicial depths can make use of the study of U -processes [Korolyuk and Borovskich, 2013]. In particular, the sample depths converge almost surely to their population counterparts. Moreover, since the set of simplices in \mathbb{R}^p forms a VC-class [Arcones and Giné, 1993], this convergence can be made uniform over \mathbb{R}^p .

Theorem 26 For any distribution P on \mathbb{R}^p , we have that

$$\begin{aligned} \sup_{x \in \mathbb{R}^p} |d_{\Delta,n}(x; P) - d_{\Delta}(x; P)| &\xrightarrow[n \rightarrow \infty]{} 0 \quad \text{almost surely,} \\ \sup_{x \in \mathbb{R}^p} |d_{\sigma,k(n,p)}(x; P) - d_{\sigma}(x; P)| &\xrightarrow[n \rightarrow \infty]{} 0 \quad \text{almost surely and} \\ \sup_{x \in \mathbb{R}^p} |d_{\sigma,n}(x; P) - d_{\sigma}(x; P)| &\xrightarrow[n \rightarrow \infty]{} 0 \quad \text{almost surely.} \end{aligned}$$

Corollary 27 The following statement is satisfied for (d, d_n) equal to either $(d_{\Delta}, d_{\Delta,n})$, $(d_{\sigma}, d_{\sigma,k})$ or $(d_{\sigma}, d_{\sigma,n})$.

For any distribution P on \mathbb{R}^p such that $d(\cdot; P)$ is uniquely maximized, we have that

$$\mu_n \rightarrow \mu \quad \text{almost surely}$$

with μ denoting the maximization point of $d(\cdot; P)$ and $\{\mu_n\}_n$ a sequence of points in \mathbb{R}^p such that $d_n(\mu_n; P) = \sup_{x \in \mathbb{R}^p} d_n(x; P)$.

In the following theorem, $\ell^{\infty}(\mathbb{R}^p)$ refers to the space of all bounded functions $f : \mathbb{R}^p \rightarrow \mathbb{R}$ and the convergence in law in $\ell^{\infty}(\mathbb{R}^p)$ (denoted by \rightsquigarrow) is in the sense of Hoffmann-Jørgensen [Massé, 2002]. Furthermore, using the notation of Definition 23, $h_x(X_{i_1}, \dots, X_{i_p}, X_{j_{1,1}}, \dots, X_{j_{p,p-1}}) := \mathbf{I}(x \in \Delta[Y_{i_1, j_{1,1}}, \dots, j_{1,p-1}}, \dots, Y_{i_p, j_{p,1}, \dots, j_{p,p-1}}])$.

Theorem 28 For any distribution P on \mathbb{R}^p ,

- (i) $\{\sqrt{n}(d_{\Delta,n}(x; P) - d_{\Delta}(x; P)) : x \in \mathbb{R}^p\} \xrightarrow[n \rightarrow \infty]{} \{(p+1)G_P^{\Delta}(x) : x \in \mathbb{R}^p\}$
- (ii) $\{\sqrt{k(n,p)}(d_{\sigma,k(n,p)}(x; P) - d_{\sigma}(x; P)) : x \in \mathbb{R}^p\} \xrightarrow[n \rightarrow \infty]{} \{(p+1)G_{P_{\sigma}}(x) : x \in \mathbb{R}^p\}$
- (iii) $\{\sqrt{n}(d_{\sigma,n}(x; P) - d_{\sigma}(x; P)) : x \in \mathbb{R}^p\} \xrightarrow[n \rightarrow \infty]{} \{(p+1)^2 G_P^{\sigma}(x) : x \in \mathbb{R}^p\}$.

G_P^{Δ} , $G_{P_{\sigma}}$ and G_P^{σ} are centered Gaussian process with covariance function

$$\mathbb{E}[G(x)G(y)] = \int g_x(z)g_y(z) dP(z) - \int g_x(z) dP(z) \int g_y(z) dP(z)$$

where $g_x(z) = \int \mathbf{I}(x \in \Delta_{\sigma}[x_1, \dots, x_p, z]) dP(x_1) \dots dP(x_p)$ in (i), $g_x(z) = \int \mathbf{I}(x \in \Delta[x_1, \dots, x_p, z]) dP_{\sigma}(x_1) \dots dP_{\sigma}(x_p)$ in (ii) and $g_x(z) = \frac{1}{p+1} \int h_x(z, x_2, \dots, x_{(p+1)^2}) dP(x_2) \dots dP(x_{(p+1)^2}) + \frac{p}{p+1} \int h_x(x_1, \dots, x_{p^2+2p}, z) dP(x_1) \dots dP(x_{p^2+2p})$ in (iii).

4 Generalization of the halfspace depth

The halfspace depth [Tukey, 1975] of a point $x \in \mathbb{R}^p$ with respect to a distribution P on \mathbb{R}^p is $d_H(x; P) := \inf_{u \in S^{p-1}} P(H_{u,x})$, where $H_{u,x} := \{y \in \mathbb{R}^p : \langle u, x \rangle \leq \langle u, y \rangle\}$ is the halfspace determined by the vector $u \in S^{p-1}$ and the point $x \in \mathbb{R}^p$. S^{p-1} denotes the unit sphere in \mathbb{R}^p and $\langle \cdot, \cdot \rangle$ is the standard inner product in \mathbb{R}^p . The objective of this section is to modify the halfspace depth in a manner that the depth values of the points in \mathbb{R}^p that are outside the convex hull of the support of P are not necessarily zero. For that we propose to compute the infimum of the probability of an enlarged halfspace. Other options are possible, as shown in previous section with the simplicial depth.

Definition 29 *Given $\eta > 0$, the η -halfspace depth of a point $x \in \mathbb{R}^p$ with respect to a distribution P on \mathbb{R}^p is*

$$d_\eta(x; P) := \inf_{u \in S^{p-1}} P(H_{u,x}^\eta),$$

where $H_{u,x}^\eta := \{y \in \mathbb{R}^p : \langle u, x \rangle \leq \langle u, y \rangle + \eta\}$.

4.1 Properties of the η -halfspace depth

Proposition 30 below studies the η -halfspace depth as a function of η ; Theorems 32 and 33 and the corollary below does it as a function of x .

Proposition 30 *The η -halfspace depth is, as a function of η , monotonically nondecreasing and continuous on the right. If computed with respect to a smooth distribution, it is also continuous and*

$$d_\eta(x; P) = \min_{u \in S^{p-1}} P(H_{u,x}^\eta)$$

for any distribution P on \mathbb{R}^p and $x \in \mathbb{R}^p$.

The following definition generalizes the concept of halfspace symmetry in multivariate spaces. We use this generalization in studying the properties of the η -halfspace depth in Theorem 32.

Definition 31 *Given $\eta > 0$ and $q \in [0, 1]$, a distribution P on \mathbb{R}^p is q - η -halfspace symmetric about $\mu \in \mathbb{R}^p$ iff $P(H_{u,\mu}^\eta) \geq q$ for all $u \in S^{p-1}$ and it does not exist a point $x \in \mathbb{R}^p$ and a $q^* > q$ such that $P(H_{u,x}^\eta) \geq q^*$ for all $u \in S^{p-1}$.*

Theorem 32 *The η -halfspace depth satisfies the properties of: (i) rigid body invariance, (ii) maximality at the center with respect to the notion of q - η -halfspace symmetry, (iii) monotonicity relative to the deepest point, (iv) vanishing at infinity and (v) upper semicontinuity as a function of x . Additionally, if computed with respect to a smooth distribution, it is also (vi) continuous as a function of x .*

Theorem 33 *The depth trimmed regions based on the η -halfspace depth are (i) rigid-body equivariant, (ii) nested, (iii) connected, (iv) compact and (v) convex.*

Corollary 34 *For any distribution P on \mathbb{R}^p , there exists at least one $\mu \in \mathbb{R}^p$ such that $d_\eta(\mu; P) = \sup_{x \in \mathbb{R}^p} d_\eta(x; P)$.*

4.2 Sample η -halfspace depth and consistency property

Definition 35 Let P be a given distribution on \mathbb{R}^p and P_n the empirical distribution associated to a sample X_1, \dots, X_n of random draws taken from P . For any $x \in \mathbb{R}^p$,

$$d_{\eta,n}(x; P) := \inf_{u \in S^{p-1}} \frac{1}{n} \sum_{i=1}^n \mathbf{I}(X_i \in H_{u,x}^\eta).$$

Theorem 36 For any distribution P on \mathbb{R}^p , we have that

$$\sup_{x \in \mathbb{R}^p} |d_{\eta,n}(x; P) - d_\eta(x; P)| \xrightarrow[n \rightarrow \infty]{} 0 \quad \text{almost surely.}$$

Corollary 37 For any distribution P on \mathbb{R}^p such that $d_\eta(\cdot; P)$ is uniquely maximized, we have that

$$\mu_n \rightarrow \mu \quad \text{almost surely}$$

with μ denoting the maximization point of $d_\eta(\cdot; P)$ and $\{\mu_n\}_n$ a sequence of points in \mathbb{R}^p such that $d_{\eta,n}(\mu_n; P) = \sup_{x \in \mathbb{R}^p} d_{\eta,n}(x; P)$.

5 Proofs

Unless specified otherwise, P is the probability measure over the Borel sets of \mathbb{R}^p .

Proof of Proposition 1. The case of X being symmetric about μ with respect to either spherical, elliptical or central symmetry, is addressed below in the proofs of Proposition 2 and 3 ($n = 1$).

Let X be angularly symmetric about μ . According to Zuo and Serfling [2000b, Theorem 2.2], angular symmetry is equivalent to $\mathbb{P}(u^\top(X - \mu) \geq 0) = \mathbb{P}(u^\top(\mu - X) \geq 0)$ for all $u \in S^{p-1}$. Denote $E_u^1 := [u^\top(X - \mu) \geq 0]$ and $E_u^2 := [u^\top(\mu - X) \geq 0]$ for any $u \in S^{p-1}$. Let $\lambda > 0$. Multiplying by λ on both sides of the inequality in E_u^1 and E_u^2 and adding and subtracting b to X , we have that $E_u^1 = [u^\top((\lambda X + b) - (\lambda\mu + b)) \geq 0]$ and $E_u^2 = [u^\top((\lambda\mu + b) - (\lambda X + b)) \geq 0]$. Due to $\mathbb{P}(E_u^1) = \mathbb{P}(E_u^2)$ and the arbitrary of u , we get that $\lambda X + b$ is angularly symmetric about $\lambda\mu + b$. The proof follows analogously for $\lambda < 0$, as we obtain $E_u^1 = [u^\top((\lambda\mu + b) - (\lambda X + b)) \geq 0]$ and $E_u^2 = [u^\top((\lambda X + b) - (\lambda\mu + b)) \geq 0]$. If $\lambda = 0$, $\lambda X + b$ is the degenerate random variable b , which, clearly, is angularly symmetric about $\lambda\mu + b = b$.

Let X be halfspace symmetric about μ . According to Zuo and Serfling [2000b, Theorem 2.4], X is halfspace symmetric about μ if and only if $\text{Med}(u^\top X) = u^\top \mu$ for all $u \in S^{p-1}$, with $\text{Med}(\cdot)$ denoting the median function. For any $\lambda \in \mathbb{R}$ and $b \in \mathbb{R}^p$, we have that $\text{Med}(u^\top(\lambda X + b)) = \lambda \text{Med}(u^\top X) + u^\top b = \lambda u^\top \mu + u^\top b = u^\top(\lambda\mu + b)$, where the first equality is thanks to the median is a homogeneous function. Thus, $\lambda X + b$ is halfspace symmetric about $\lambda\mu + b$. ■

Proof of Proposition 2. Let X_i be elliptically symmetric about μ for each $i = 1, \dots, n$. As X_1, \dots, X_n are identically distributed, there exists a nonsingular matrix V such that VX_i is spherically symmetric about $V\mu$ for all $i = 1, \dots, n$.

Thus, $U(VX_i - V\mu) \stackrel{d}{=} (VX_i - V\mu)$ for any orthonormal matrix U and $i = 1, \dots, n$. Given $\lambda \in \mathbb{R}$ and $b \in \mathbb{R}^p$, let us denote $Y := \sum_{i=1}^n \lambda_i X_i + b$ and $\tilde{\mu} := \sum_{i=1}^n \lambda_i \mu_i + b$. Thus,

$$\begin{aligned} U(VY - V\tilde{\mu}) &\stackrel{d}{=} U\left(\sum_{i=1}^n \lambda_i (VX_i - V\mu)\right) \stackrel{d}{=} \sum_{i=1}^n \lambda_i U(VX_i - V\mu) \\ &\stackrel{d}{=} \sum_{i=1}^n \lambda_i (VX_i - V\mu) \stackrel{d}{=} VY - V\tilde{\mu}, \end{aligned}$$

for any orthonormal matrix U . Then, Y is elliptically symmetric about $\tilde{\mu}$.

The cases of spherical and central symmetry are addressed below in the proof of Proposition 3. ■

Proof of Proposition 3. Given $\lambda \in \mathbb{R}$ and $b \in \mathbb{R}^p$, let us denote $Y := \sum_{i=1}^n \lambda_i X_i + b$ and $\tilde{\mu} := \sum_{i=1}^n \lambda_i \mu_i + b$. Let X_i be spherically symmetric about μ_i for $i = 1, \dots, n$. Then, for any orthonormal matrix U

$$U(Y - \tilde{\mu}) \stackrel{d}{=} U\left(\sum_{i=1}^n \lambda_i (X_i - \mu_i)\right) \stackrel{d}{=} \sum_{i=1}^n \lambda_i U(X_i - \mu_i) \stackrel{d}{=} \sum_{i=1}^n \lambda_i (X_i - \mu_i) \stackrel{d}{=} Y - \tilde{\mu},$$

which implies that Y is spherically symmetric about $\tilde{\mu}$.

According to Zuo and Serfling [2000b, Lemma 2.1], a random variable X is centrally symmetric about $\mu \in \mathbb{R}^p$ if and only if $u^\top(X - \mu) \stackrel{d}{=} u^\top(\mu - X)$ for all $u \in S^{p-1}$. Let X_i be centrally symmetric about μ_i for $i = 1, \dots, n$. Then, Y is centrally symmetric about $\tilde{\mu}$ as $u^\top(Y - \tilde{\mu}) \stackrel{d}{=} \sum_{i=1}^n \lambda_i u^\top(X_i - \mu_i) \stackrel{d}{=} \sum_{i=1}^n \lambda_i u^\top(\mu_i - X_i) \stackrel{d}{=} u^\top(\tilde{\mu} - Y)$. ■

Proof of Corollary 4. The proof follows directly from Proposition 3 as elliptical symmetry implies central symmetry. ■

Proof of Theorem 9. Recall that a distribution P on \mathbb{R}^p (or a random variable $X \sim P$) is continuous if $P(\{x\}) = 0$ for all $x \in \mathbb{R}^p$ and absolutely continuous if $P(A) = 0$ for any Lebesgue measure 0 set $A \subset \mathbb{R}^p$. Since P_σ is the distribution of $\sigma X_1 + \frac{1-\sigma}{p+1} \sum_{j=1}^{p+1} X_j$ where X_1, \dots, X_{p+1} are independent and identically distributed random variables with distribution P , it is enough to show that a linear combination of continuous (or respectively absolutely continuous or smooth) random variables is continuous (or respectively absolutely continuous or smooth). For this, it suffices to prove that: (i) if $X \sim P$ is continuous (or respectively absolutely continuous or smooth), then λX is continuous (or respectively absolutely continuous or smooth) for any $\lambda \in \mathbb{R} \setminus \{0\}$; and (ii) if $X \sim P$ and $Y \sim Q$ are continuous (or respectively absolutely continuous or smooth), then the sum $X + Y$ is continuous (or respectively absolutely continuous or smooth).

For (i), observe that $\lambda X \sim P^\lambda$ where $P^\lambda(B) := P(\frac{1}{\lambda}B)$ for all measurable subsets $B \subset \mathbb{R}^p$, while for (ii), notice that $X + Y$ has distribution $P * Q$ such that $(P * Q)(B) = \int P(B + \{y\}) dQ(y)$ for $B \subset \mathbb{R}^p$ measurable. In both cases, the result follows by considering sets B of a specific form: if P is continuous take

$B = \{x\}$ for $x \in \mathbb{R}^p$, if P is absolutely continuous consider Lebesgue measure 0 sets and if P is smooth consider hyperplanes in \mathbb{R}^p . ■

Proof of Theorem 10. It is a direct consequence of Proposition 2. ■

Proof of Proposition 11. As P_X is centrally symmetric about μ , we have that $\mathbb{E}(X) - \mu = \mathbb{E}(X - \mu) = \mathbb{E}(\mu - X) = \mu - \mathbb{E}(X)$, which implies that $\mathbb{E}(X) = \mu$. ■

Proof of Proposition 12. Let us denote $Y := \sum_{i=1}^{p+1} \lambda_i X_i$ and $\mu := \mathbb{E}(X_1)$. Due to the X_i 's are identically distributed and $\sum_{i=1}^{p+1} \lambda_i = 1$, $\mathbb{E}(Y) = \sum_{i=1}^{p+1} \lambda_i \mathbb{E}(X_i) = \mu$. Then,

$$\begin{aligned} \mathbb{E}((Y - \mu)(Y - \mu)^\top) &= \mathbb{E}\left(\left(\sum_{i=1}^{p+1} \lambda_i (X_i - \mu)\right) \left(\sum_{i=1}^{p+1} \lambda_i (X_i - \mu)\right)^\top\right) = \\ &= \sum_{i=1}^{p+1} \lambda_i^2 \mathbb{E}((X_i - \mu)(X_i - \mu)^\top) = \left(\sigma^2 + \frac{1-\sigma^2}{p+1}\right) \Sigma, \end{aligned}$$

where we have made use of the independency of the X_i 's and that $\sum_{i=1}^{p+1} \lambda_i^2 = \sigma^2 + \frac{1-\sigma^2}{p+1}$. ■

The next lemma shows that simplices are nested, which is required for the proof of Proposition 14 and 24.

Lemma 38 For all $x_1, \dots, x_{p+1} \in \mathbb{R}^p$ and scalars $\sigma_* \geq \sigma \geq 1$, we have that $\Delta_{\sigma_*}[x_1, \dots, x_{p+1}] \supset \Delta_\sigma[x_1, \dots, x_{p+1}]$.

Proof of Lemma 38 . Let $y \in \Delta_\sigma[x_1, \dots, x_{p+1}]$, then $\Delta_\sigma[x_1, \dots, x_{p+1}] = \Delta[y_1, \dots, y_{p+1}]$ for

$$y_i := \sigma x_i + (1 - \sigma)/(p + 1) \sum_{j=1}^{p+1} x_j, \text{ with } i = 1, \dots, p + 1. \quad (1)$$

Due to Liu [1990, Equation (1.8)], there exist $\alpha_1, \dots, \alpha_{p+1} \geq 0$ with $\alpha_1 + \dots + \alpha_{p+1} = 1$ such that $y = \alpha_1 y_1 + \dots + \alpha_{p+1} y_{p+1}$; which by (1) results in

$$y = \sigma \left(\sum_{i=1}^{p+1} \alpha_i x_i - \frac{1}{p+1} \sum_{i=1}^{p+1} x_i \right) + \frac{1}{p+1} \sum_{i=1}^{p+1} x_i.$$

Multiplying and dividing by σ^* the first term of the sum,

$$\begin{aligned} y &= \sigma^* \left(\sum_{i=1}^{p+1} \left(\frac{\sigma}{\sigma^*} \alpha_i \right) x_i - \left(\frac{\sigma}{\sigma^*} \right) \frac{1}{p+1} \sum_{i=1}^{p+1} x_i \right) + \frac{1}{p+1} \sum_{i=1}^{p+1} x_i \\ &= \sigma^* \left(\sum_{i=1}^{p+1} \alpha_i^* x_i - \frac{1}{p+1} \sum_{i=1}^{p+1} x_i \right) + \frac{1}{p+1} \sum_{i=1}^{p+1} x_i \end{aligned} \quad (2)$$

with $\alpha_i^* := \frac{\sigma}{\sigma^*} \alpha_i + \frac{\sigma^* - \sigma}{\sigma^*}$ for $i = 1, \dots, p+1$. Observe that $\alpha_i^* \geq 0$ and $\sum_{i=1}^{p+1} \alpha_i^* = 1$. We rewrite equation (2) as $y = \alpha_1^* y_1^* + \dots + \alpha_{p+1}^* y_{p+1}^*$ where $y_i^* = \sigma^* x_i + (1 - \sigma^*)/(p + 1) \sum_{j=1}^{p+1} x_j$ for $i = 1, 2, \dots, p + 1$. Thus, $y \in \Delta[y_1^*, \dots, y_{p+1}^*]$. The proof finishes because $\Delta_{\sigma^*}[x_1, \dots, x_{p+1}] = \Delta[y_1^*, \dots, y_{p+1}^*]$ by the definition of enlarged simplex. ■

Proof of Proposition 14. The simplex enlarged simplicial depth is monotonically non-decreasing as a function of σ as a direct consequence of above Lemma 38.

We prove next the continuity on the right and the continuity for smooth P of the σ -simplicial depth. Let $\sigma > 1$ and $\{\sigma_n\}_{n=1}^{\infty}$ be a sequence of real numbers that converges to σ . Note that in Definition 5 Δ depends on σ , $\Delta = \Delta_\sigma$ and for any $n \in \mathbb{N}$, $x \in \mathbb{R}$ and P on \mathbb{R}^p , $|d_{\Delta_{\sigma_n}}(x; P) - d_{\Delta_\sigma}(x; P)| \leq \int |g_n(x_1, \dots, x_{p+1}) - g(x_1, \dots, x_{p+1})| dP(x_1) \dots dP(x_{p+1})$ where $g(x_1, \dots, x_{p+1}) := \mathbf{I}(x \in \Delta_\sigma[x_1, \dots, x_{p+1}])$ and analogously for g_n , $n \geq 1$. Clearly $\{g_n\}_{n=1}^{\infty}$ is measurable and bounded by 1. Moreover, for (x_1, \dots, x_{p+1}) fixed we have two possibilities: (i) if x is not on the boundary of $\Delta_\sigma[x_1, \dots, x_{p+1}]$, there exists an $\epsilon > 0$ and $N \in \mathbb{N}$ such that $|\sigma - \sigma_n| < \epsilon$ and $g_n(x_1, \dots, x_{p+1}) = g(x_1, \dots, x_{p+1})$ for all $n \geq N$; (ii) if x is on the boundary of $\Delta_\sigma[x_1, \dots, x_{p+1}]$, $\lim_{\sigma_n \uparrow \sigma} \mathbf{I}(x \in \Delta_{\sigma_n}[x_1, \dots, x_{p+1}]) = 0$ and $\lim_{\sigma_n \downarrow \sigma} \mathbf{I}(x \in \Delta_{\sigma_n}[x_1, \dots, x_{p+1}]) = 1$. Therefore, if $\{\sigma_n\}_{n=1}^{\infty}$ converges from above to σ , the corresponding sequence of functions $\{g_n\}_{n=1}^{\infty}$ convergence pointwise to g and because of the Lebesgue's dominated convergence theorem, the distribution enlarged σ -simplicial depth is right continuous.

Let P be smooth. The set $\{(x_1, \dots, x_{p+1}) \in \mathbb{R}^p \times \dots \times \mathbb{R}^p : x \in \partial\Delta_\sigma[x_1, \dots, x_{p+1}]\}$ has measure 0. Hence, h_n converges pointwise to h almost everywhere. The result follows again from Lebesgue's dominated convergence theorem.

The proof of the continuity of the distribution enlarged σ -simplicial depth for smooth P is similar. Each P_σ , and P_{σ_n} , is replaced by $p+1$ P 's, so that the dependence on σ is not in the probability distribution but only in the integrand (see Definition 6). For any $n \in \mathbb{N}$, $x \in \mathbb{R}$ and P on \mathbb{R}^p , $|d_{\sigma_n}(x; P) - d_\sigma(x; P)| \leq \int |h_n(x_1, \dots, x_{(p+1)^2}) - h(x_1, \dots, x_{(p+1)^2})| dP(x_1) \dots dP(x_{(p+1)^2})$ where $h(x_1, \dots, x_{(p+1)^2}) := \mathbf{I}(x \in \Delta^\sigma)$ with

$$\Delta^\sigma := \Delta \left[\sigma x_1 + \frac{1-\sigma}{p+1} \sum_{j=1}^{p+1} x_j, \dots, \sigma x_{1+p(p+1)} + \frac{1-\sigma}{p+1} \sum_{j=1+p(p+1)}^{(p+1)^2} x_j \right];$$

and analogously for h_n , $n \geq 1$. The result follows again from Lebesgue's dominated convergence theorem and the almost sure pointwise convergence of the sequence $\{h_n\}_{n=1}^{\infty}$ to h .

We prove next the monotonicity of the distribution enlarged sigma simplicial depth. If P has density $f(x) = \kappa g((x - \mu)^\top \Sigma^{-1}(x - \mu))$ from Zuo and Serfling [2000c, Theorem 3.3] we see that $d_\sigma(x; P) = h((x - \mu)^\top \Sigma_\sigma^{-1}(x - \mu))$, where h is a nonincreasing function and $\Sigma_\sigma = \left(\sigma^2 + \frac{1-\sigma^2}{p+1}\right) \Sigma$ is as in Proposition 12. Therefore, for any scalars $\sigma_* \geq \sigma \geq 1$, $d_{\sigma_*}(x; P) \geq d_\sigma(x; P)$. ■

Proof of Theorem 15. (i) The affine invariance property follows from Liu [1990, Equation (1.8)] and the fact that, for any $p \times p$ nonsingular matrix A and p dimensional vector b , $Ay + b \in \Delta[Ay_1 + b, \dots, Ay_{p+1} + b]$ if and only if $y \in \Delta[y_1, \dots, y_{p+1}]$.

(ii) For the vanishing at infinity property, observe that

$$\begin{aligned} \lim_{\|x\| \rightarrow \infty} d_\sigma(x; P) &\leq \limsup_{\|x\| \rightarrow \infty} d_\sigma(x; P) \\ &\leq \int \limsup_{\|x\| \rightarrow \infty} \mathbf{I}(x \in \Delta_\sigma[x_1, \dots, x_{p+1}]) dP(x_1) \dots dP(x_{p+1}) = 0, \end{aligned}$$

because of Lebesgue's dominated convergence theorem.

(iii) For the upper semicontinuity property, let $x^* \in \mathbb{R}^p$ and note that

$$\begin{aligned} \limsup_{x \rightarrow x^*} d_\sigma(x; P) &\leq \int \limsup_{x \rightarrow x^*} \mathbf{I}(x \in \Delta_\sigma[x_1, \dots, x_{p+1}]) dP(x_1) \dots dP(x_{p+1}) \\ &\leq \int \mathbf{I}(x^* \in \Delta_\sigma[x_1, \dots, x_{p+1}]) dP(x_1) \dots dP(x_{p+1}) \\ &= d_\sigma(x^*; P). \end{aligned}$$

(iv) Finally, let P be smooth, then

$$\begin{aligned} \liminf_{x \rightarrow x^*} d_\sigma(x; P) &\geq \int \liminf_{x \rightarrow x^*} \mathbf{I}(x \in \Delta_\sigma[x_1, \dots, x_{p+1}]) dP(x_1) \dots dP(x_{p+1}) \\ &= d_\sigma(x^*; P). \end{aligned}$$

■

Proof of Proposition 16. For any $x \in \mathbb{R}$ and P on \mathbb{R} ,

$$\begin{aligned} d_\Delta(x; P) &= \\ &= \int \mathbf{I}\left(\frac{1+\sigma}{2}x_1 + \frac{1-\sigma}{2}x_2 \leq x \leq \frac{1-\sigma}{2}x_1 + \frac{1+\sigma}{2}x_2\right) dP(x_1)dP(x_2) \\ &+ \int \mathbf{I}\left(\frac{1-\sigma}{2}x_1 + \frac{1+\sigma}{2}x_2 \leq x \leq \frac{1+\sigma}{2}x_1 + \frac{1-\sigma}{2}x_2\right) dP(x_1)dP(x_2) \\ &- \int \mathbf{I}(x_1 = x_2 = x) dP(x_1)dP(x_2). \end{aligned}$$

For any $x \in \mathbb{R}$, let us denote

$$\begin{aligned} S_1^+(x) &:= \left\{ (x_1, x_2) \in \mathbb{R}^2 : \frac{1+\sigma}{2}x_1 + \frac{1-\sigma}{2}x_2 \leq x \right\}, \\ S_2^+(x) &:= \left\{ (x_1, x_2) \in \mathbb{R}^2 : \frac{1-\sigma}{2}x_1 + \frac{1+\sigma}{2}x_2 \geq x \right\}, \\ S_1^-(x) &:= \left\{ (x_1, x_2) \in \mathbb{R}^2 : \frac{1+\sigma}{2}x_1 + \frac{1-\sigma}{2}x_2 \geq x \right\}, \\ S_2^-(x) &:= \left\{ (x_1, x_2) \in \mathbb{R}^2 : \frac{1-\sigma}{2}x_1 + \frac{1+\sigma}{2}x_2 \leq x \right\}, \end{aligned}$$

$S^+(x) := S_1^+(x) \cap S_2^+(x)$ and $S^-(x) := S_1^-(x) \cap S_2^-(x)$. Then,

$$d_\Delta(x; P) = \int_{S^+(x)} dP(x_1)dP(x_2) + \int_{S^-(x)} dP(x_1)dP(x_2) - \int_{\{(x,x)\}} dP(x_1)dP(x_2).$$

Without loss of generality, let us assume that $0 \in S$. We consider the case $x \geq y > 0$. The proof of the case $x \leq y < 0$ is analogous. Thus,

$$\begin{aligned}
d_{\Delta}(y; P) - d_{\Delta}(x; P) &= \\
&= \int_{S^+(y) \setminus S_2^+(x)} dP(x_1)dP(x_2) + \int_{S^-(y) \setminus S_1^-(x)} dP(x_1)dP(x_2) \\
&\quad - \int_{\{(y,y)\}} dP(x_1)dP(x_2) - \int_{S^+(x) \setminus S_1^+(y)} dP(x_1)dP(x_2) \\
&\quad - \int_{S^-(x) \setminus S_2^-(y)} dP(x_1)dP(x_2) + \int_{\{(x,x)\}} dP(x_1)dP(x_2).
\end{aligned}$$

Notice that $S^+(x) \setminus S_1^+(y)$ and $S^-(x) \setminus S_2^-(y)$ have no intersection with $S \times S$. Hence, their corresponding probability is zero. Furthermore $\{(y, y)\}$ is a subset of both $S^+(y) \setminus S_2^+(x)$ and $S^-(y) \setminus S_1^-(x)$. All this implies that $d_{\Delta}(y; P) - d_{\Delta}(x; P) \geq 0$. ■

Proof of Theorem 17. As the distribution enlarged σ -simplicial depth with respect to a distribution P is the simplicial depth with respect to the corresponding distribution P_{σ} , properties (i) and (ii) follow from Liu [1990, Equations (1.8) and (1.9), Theorem 1] and the, above, proof of Theorem 15. The proofs of properties (iii) and (iv) are similar to that of Theorem 15 (see also Liu [1990, Theorem 2]). Observe that thanks to Theorem 9, if P is smooth, then P_{σ} is smooth. Finally, if P is centrally symmetric then, because of Theorem 10, P_{σ} is centrally symmetric about the same point. Therefore, properties (v) and (vi) follow from Liu [1990, Theorem 3]. ■

Proof of Theorem 18. (i) and (ii) follow directly from Zuo and Serfling [2000c, Theorem 3.1]. For the distribution enlarged σ -simplicial depth, (iii) holds because point (iv) of Theorem 17 implies that the depth trimmed regions are closed and point (ii) of Theorem 17 that implies that the depth trimmed regions are bounded. For the simplex enlarged σ -simplicial depth, the proof is the same using Theorem 15. (iv) is a consequence of point (vi) of Theorem 17 and point (c) of Zuo and Serfling [2000c, Theorem 3.1]. ■

Proof of Corollary 19. This is a direct consequence of Proposition 18. For the proof see Rousseeuw and Ruts [1999, Proposition 7]. ■

Proof of Proposition 24. $d_{\Delta, n}(x; P)$ is an average of indicators of the form $\mathbf{I}(x \in \Delta_{\sigma}[x_1, \dots, x_{p+1}])$ for $x_1, \dots, x_{p+1} \in \mathbb{R}^p$. Then, the result follows from Lemma 38. ■

Proof of Proposition 25. For any distribution P on \mathbb{R}^{p-1} , $d_{\Delta, n}(\cdot; P)$ and $d_{\sigma, k}(\cdot; P)$ are clearly U -statistic of order p with symmetric kernels for the estimation of $d_{\Delta}(\cdot; P)$ and $d_{\sigma}(\cdot; P)$, respectively. We see also that $d_{\sigma, n}(x; P)$ is a U -statistics of order p^2 with symmetric kernel K_x , given below, for the estimation of $d_{\sigma}(\cdot; P)$. In fact, it can be written in the form

$$d_{\sigma, n}(x; P) = \binom{n}{p^2}^{-1} \sum_{1 \leq l_1 < \dots < l_{p^2} \leq n} K_x(X_{l_1}, \dots, X_{l_{p^2}}),$$

where

$$K_x(X_{l_1}, \dots, X_{l_{p^2}}) = \frac{p!((p-1)!)^p}{p^{2p}} \sum_A h_x(X_{i_1}, \dots, X_{i_p}, X_{j_{1,1}}, \dots, X_{j_{p,p-1}}).$$

$A := \{(i_1, \dots, i_p, j_{1,1}, \dots, j_{p,p-1}) \in G(l_1, \dots, l_{p^2})\}$ with $G(l_1, \dots, l_{p^2})$ the set of all possible p^2 -tuples $(i_1, \dots, i_p, j_{1,1}, \dots, j_{p,p-1})$ given by splitting the indices l_1, \dots, l_{p^2} into p ordered groups, the first of size p and the remaining p of size $p-1$ and $h_x(X_{i_1}, \dots, X_{i_p}, X_{j_{1,1}}, \dots, X_{j_{p,p-1}}) = \mathbf{I}(x \in \Delta[Y_{i_1, j_{1,1}}, \dots, j_{1,p-1}}, \dots, Y_{i_p, j_{p,1}}, \dots, j_{p,p-1}}])$.

■

Proof of Theorem 26. By Proposition 25, the sample depths are U-statistics for the estimation of their population counterpart. Moreover the class of functions indexing each of them are collections of indicators of a VC-class of sets (i. e. simplices in \mathbb{R}^{p-1}). For the almost sure uniform convergence of $d_{\Delta, n}(\cdot, P)$ to $d_{\Delta}(\cdot, P)$, observe that the only difference with the classical simplicial depth is the rescaling of the simplices. Therefore, Arcones and Giné [1993, Corollary 6.7] holds. The result follows from Corollary 3.3 therein. Due to $d_{\sigma, k(n,p)}(\cdot, P) = d_{k(n,p)}(\cdot, P_{\sigma})$ is the classical sample simplicial depth based on k independent random draws with distribution P_{σ} , its almost sure uniform convergence to $d_{\sigma}(\cdot, P)$ follows from Arcones and Giné [1993, Corollary 6.8]. Finally, the convergence of $d_{\sigma, n}(\cdot, P)$ to $d_{\sigma}(\cdot, P)$ follows from Arcones and Giné [1993, Corollary 3.3] along with a slight modification of Corollary 6.7 there, in order to adapt it to the class of functions $\{h_x : x \in \mathbb{R}^{p-1}\}$, with h_x is as in the proof of Proposition 25. ■

Proof of Corollary 27. The σ -simplicial depths $d_{\Delta}(\cdot, P)$ and $d_{\sigma}(\cdot, P)$ are upper semicontinuous and vanish at infinity because of Theorem 15 and 17, respectively. Furthermore, Theorem 26 implies that, for either of the three cases of (d, d_n) , $d_n(\cdot; P)$ converges uniformly almost surely to $d(\cdot; P)$. Therefore, the proof of the almost sure convergence of μ_n to μ is analogous to that of Arcones and Giné [1993, Theorem 6.9]. ■

Proof of Theorem 28. It follows from Arcones and Giné [1993, Theorem 4.9]. In particular, $g_x(z) = \int k_x(x_1, \dots, x_{m-1}, z) dP(x_1) \dots dP(x_{m-1})$, where $m = p + 1$ for (i) and (ii), $m = (p + 1)^2$ for (iii) and k_x is the kernel of the corresponding U-statistic. This gives directly g_x for (i) and (ii), while for (iii)

$$\begin{aligned} g_x(z) &= \int K_x(x_1, \dots, x_{p^2+p}, z) dP(x_1) \dots dP(x_{m-1}) \\ &= \frac{1}{p+1} \int h_x(z, x_2, \dots, x_{(p+1)^2}) dP(x_2) \dots dP(x_{(p+1)^2}) \\ &\quad + \frac{p}{p+1} \int h_x(x_1, \dots, x_{p^2+2p}, z) dP(x_1) \dots dP(x_{p^2+2p}) \end{aligned}$$

where K_x is as in the proof of Proposition 25. ■

For P smooth, the following lemma is required to prove continuity of the η -halfspace depth as a function of either η or x . We make use of it in Proposition 30 and Theorem 32.

Lemma 39 *If P is smooth, then the function*

$$\begin{aligned} [0, \infty) \times S^{p-1} \times \mathbb{R}^p &\rightarrow [0, 1] \\ (\eta, u, x) &\mapsto P(H_{u,x}^\eta) \end{aligned}$$

is continuous.

Proof of Lemma 39. Let $\{\eta_n\}_{n=1}^\infty \subset [0, \infty)$, $\{u_n\}_{n=1}^\infty \subset S^{p-1}$ and $\{x_n\}_{n=1}^\infty \subset \mathbb{R}^p$ such that $\eta_n \rightarrow \eta$, $u_n \rightarrow u$ and $x_n \rightarrow x$ for $n \rightarrow \infty$. Clearly,

$$|P(H_{u_n, x_n}^{\eta_n}) - P(H_{u,x}^\eta)| \leq \int_{\mathbb{R}^p} |\mathbf{I}(z \in H_{u_n, x_n}^{\eta_n}) - \mathbf{I}(z \in H_{u,x}^\eta)| dP(z).$$

Furthermore, if z does not belong to the border of $H_{u,x}^\eta$, there exists $N \in \mathbb{N}$ such that $\mathbf{I}(z \in H_{u_n, x_n}^{\eta_n}) = \mathbf{I}(z \in H_{u,x}^\eta)$ for all $n \geq N$. Due to the set $\{z \in \mathbb{R}^p : z \in \partial H_{u,x}^\eta\}$ has probability 0, the result follows from Lebesgue's dominated convergence theorem. ■

Proof of Proposition 30. The function $\eta \mapsto d_\eta(x; P) = \inf_{u \in S^{p-1}} P(H_{u,x}^\eta)$ is monotonically nondecreasing due to, for all $u \in S^{p-1}$ and scalars $\eta^* \geq \eta \geq 0$, it is obtained that $H_{u,x}^{\eta^*} \supset H_{u,x}^\eta$. For the continuity on the right, we make use of the fact that for monotonically nondecreasing functions on \mathbb{R} it is equivalent right continuity and upper semicontinuity (see the Remark after Theorem 1.1 in Kardaun [2005]). Let $\{\eta_n\}_{n=1}^\infty$ be a sequence of real numbers converging from above to η . Then, for $x \in \mathbb{R}^p$ and $u \in S^{p-1}$,

$$\lim_{n \rightarrow \infty} |P(H_{u,x}^{\eta_n}) - P(H_{u,x}^\eta)| \leq \lim_{n \rightarrow \infty} \int_{\mathbb{R}^p} |\mathbf{I}(z \in H_{u,x}^{\eta_n}) - \mathbf{I}(z \in H_{u,x}^\eta)| dP(z) = 0$$

because of the Lebesgue's dominated convergence theorem and the fact that $\lim_{n \rightarrow \infty} \mathbf{I}(z \in H_{u,x}^{\eta_n}) = \mathbf{I}(z \in H_{u,x}^\eta)$. The results follows from the fact that the infimum of upper semicontinuous functions is upper semicontinuous. If P is smooth, the function $(u, \eta) \mapsto P(H_{u,x}^\eta)$ is continuous for each $x \in \mathbb{R}^p$ by Lemma 39. As S^{p-1} is a compact set and the infimum of continuous functions over a compact set is continuous, the function $\eta \mapsto d_\eta(x; P)$ is continuous. Furthermore, for $x \in \mathbb{R}^p$ and $\eta \geq 0$, the continuity of $u \mapsto P(H_{u,x}^\eta)$ and the compactness of S^{p-1} imply that the infimum is a minimum by the extreme value theorem. ■

Proof of Theorem 32. (i) Let us show that, for any orthonormal matrix U and any $b \in \mathbb{R}^p$, $d_\eta(Ux + b; P_{UX+b}) = d_\eta(x; P)$. By Definition 29,

$$\begin{aligned} d_\eta(Ux + b; P_{UX+b}) &= \inf_{u \in S^{p-1}} \int \mathbf{I}(Uz + b \in H_{u, Ux+b}^\eta) dP(z) \\ &= \inf_{u \in S^{p-1}} \int \mathbf{I}(\langle u, Ux + b \rangle \leq \langle u, Uz + b \rangle + \eta) dP(z) \\ &= \inf_{u \in S^{p-1}} \int \mathbf{I}(\langle u, Ux \rangle \leq \langle u, Uz \rangle + \eta) dP(z). \end{aligned}$$

By the definition of the inner product on \mathbb{R}^p and due to $U^\top = U^{-1}$, we have that, for $y \in \mathbb{R}^p$, $\langle u, Uy \rangle = \langle U^\top u, y \rangle = \langle U^{-1}u, y \rangle$. Then,

$$\begin{aligned} d_\eta(Ux + b; P_{UX+b}) &= \inf_{u \in S^{p-1}} \int \mathbf{I}(\langle U^{-1}u, x \rangle \leq \langle U^{-1}u, z \rangle + \eta) dP(z) \\ &= \inf_{u \in S^{p-1}} \int \mathbf{I}(z \in H_{U^{-1}u, x}^\eta) dP(z) = \inf_{u \in S^{p-1}} P(H_{U^{-1}u, x}^\eta). \end{aligned}$$

Finally, $\inf_{u \in S^{p-1}} P(H_{U^{-1}u, x}^\eta) = \inf_{u \in S^{p-1}} P(H_{u, x}^\eta) = d_\eta(x; P)$ thanks to $U^{-1}S^{p-1} = S^{p-1}$.

(ii) For the maximality at the center property, observe that $P(H_{u, \mu}^\eta) \geq q$ for all $u \in S^{p-1}$, by the definition of q - η -halfspace symmetry. Then $d_\eta(\mu; P) = q$. Suppose for a contradiction that there exist a point $\mu^* \neq \mu$ and $q^* > q$ such that $d_\eta(\mu^*; P) = q^*$. Then, $P(H_{u, \mu^*}^\eta) \geq q^*$ for all $u \in S^{p-1}$; contradicting the fact that P is q - η -halfspace symmetric about μ .

(iii) For the monotonicity relative to the deepest point, let $\mu \in M$ with $M := \{y \in \mathbb{R}^p : d_\eta(y; P) = \sup_{x \in \mathbb{R}^p} d_\eta(x; P)\}$. By Theorem 33 and Corollary 34, M is non-empty and convex. Let $x \in \mathbb{R}^p \setminus M$ and $\alpha \in (0, 1)$ such that $\mu + \alpha(x - \mu) \in \mathbb{R}^p \setminus M$; otherwise the result is trivial. For $u \in S^{p-1}$ with $\langle u, x - \mu \rangle < 0$ we have that $H_{u, x}^\eta \supset H_{u, \mu + \alpha(x - \mu)}^\eta \supset H_{u, \mu}^\eta$, and, therefore,

$P(H_{u, x}^\eta) \geq P(H_{u, \mu + \alpha(x - \mu)}^\eta) \geq P(H_{u, \mu}^\eta) \geq d_\mu(\mu; P)$. Hence it is enough to consider $u \in S^{p-1}$ with $\langle u, x - \mu \rangle \geq 0$. For such u 's, we have that $H_{u, x}^\eta \subset H_{u, \mu + \alpha(x - \mu)}^\eta \subset H_{u, \mu}^\eta$, and, therefore,

$$\begin{aligned} d_\eta(x; P) &= \inf_{u \in S^{p-1} : \langle u, x - \mu \rangle \geq 0} P(H_{u, x}^\eta) \leq \inf_{u \in S^{p-1} : \langle u, x - \mu \rangle \geq 0} P(H_{u, \mu + \alpha(x - \mu)}^\eta) \\ &= d_\eta(\mu + \alpha(x - \mu); P). \end{aligned}$$

(iv) Let $x \neq 0$, then $d_\eta(x; P) = \inf_{u \in S^{p-1}} P(H_{u, x}^\eta) \leq P(H_{\frac{x}{\|x\|}, x}^\eta)$. Note that

$$H_{\frac{x}{\|x\|}, x}^\eta = \left\{ y \in \mathbb{R}^p : \left\langle \frac{x}{\|x\|}, x \right\rangle \leq \left\langle \frac{x}{\|x\|}, y \right\rangle + \eta \right\} = \left\{ y \in \mathbb{R}^p : \|x\| \leq \frac{\langle x, y \rangle}{\|x\|} + \eta \right\}.$$

By the Cauchy inequality, $\langle x, y \rangle \leq \|x\| \|y\|$, and therefore

$$d_\eta(x; P) \leq P(\{y \in \mathbb{R}^p : \|x\| \leq \|y\| + \eta\}) \rightarrow 0 \text{ as } \|x\| \rightarrow \infty.$$

(v) It follows from the fact that the function $x \mapsto P(H_{u, x}^\eta)$ is upper semicontinuous for all $u \in S^{p-1}$ and the infimum of a collection of upper semicontinuous functions is upper semicontinuous. Note that, for any sequence $\{x_n\}_{n=1}^\infty$ such that $x_n \rightarrow x$ when $n \rightarrow \infty$ and for all $u \in S^{p-1}$,

$$\begin{aligned} \limsup_{x_n \rightarrow x} P(H_{u, x_n}^\eta) &= \limsup_{x_n \rightarrow x} \int_{\mathbb{R}^p} \mathbf{I}(z \in H_{u, x_n}^\eta) dP(z) \\ &\leq \int_{\mathbb{R}^p} \limsup_{x_n \rightarrow x} \mathbf{I}(z \in H_{u, x_n}^\eta) dP(z) \\ &\leq \int_{\mathbb{R}^p} \mathbf{I}(z \in H_{u, x}^\eta) dP(z) = P(H_{u, x}^\eta). \end{aligned}$$

(vi) Let P be smooth. By Lemma 39 the function $(u, x) \mapsto P(H_{u,x}^\eta)$ is continuous for all $\eta \geq 0$. As S^{p-1} is compact, the infimum over all $u \in S^{p-1}$ is also continuous. ■

The following lemma is a modification of Rousseeuw and Ruts [1999, Proposition 6] and it implies that the depth trimmed regions, D_α for $\alpha \geq 0$, are closed.

Lemma 40 *For any distribution P on \mathbb{R}^p and $\alpha > 0$*

$$D_\alpha = \cap \{H_{u,x} : u \in S^{p-1}, x \in \mathbb{R}^p \text{ and } P(\mathring{H}_{-u,x}^\eta) < \alpha\}$$

with $\mathring{H}_{-u,x}^\eta$ the interior of $H_{-u,x}^\eta$.

We also refer to $\mathring{H}_{-u,x}^\eta$ as the η -enlarged complement of $H_{u,x}$.

Proof of Lemma 40. Let $z \in D_\alpha$. As $D_\alpha = \{x \in \mathbb{R}^p : d(x; P) \geq \alpha\}$, we have that $\inf_{v \in S^{p-1}} P(H_{v,z}^\eta) \geq \alpha$, and therefore

$$P(H_{v,z}^\eta) \geq \alpha \text{ for all } v \in S^{p-1}. \quad (3)$$

Let $u \in S^{p-1}$ and $x \in \mathbb{R}^p$ such that $P(\mathring{H}_{-u,x}^\eta) < \alpha$. Suppose for a contradiction that $z \notin H_{u,x}$. Then, z is in its complement: $z \in \mathring{H}_{-u,x}$, and therefore, $H_{-u,z} \subset \mathring{H}_{-u,x}$. This implies that $P(H_{-u,z}^\eta) \leq P(\mathring{H}_{-u,x}^\eta) < \alpha$, which contradicts equation (3).

On the contrary, let $z \in \mathcal{H}_\alpha := \cap \{H_{u,x} : u \in S^{p-1}, x \in \mathbb{R}^p \text{ and } P(\mathring{H}_{-u,x}^\eta) < \alpha\}$. Suppose for a contradiction that $z \notin D_\alpha$. Then, there is a $v \in S^{p-1}$ such that $P(H_{v,z}^\eta) = \alpha_0 < \alpha$. As $H_{v,z}^\eta = \cap_{n=1}^\infty \mathring{H}_{v,z}^{\eta+\frac{1}{n}}$, we have that $\alpha_0 = P(H_{v,z}^\eta) = P(\cap_{n=1}^\infty \mathring{H}_{v,z}^{\eta+\frac{1}{n}}) = \lim_{n \rightarrow \infty} P(\mathring{H}_{v,z}^{\eta+\frac{1}{n}})$. Therefore, there exists $m \in \mathbb{N}$ such that $P(\mathring{H}_{v,z}^{\eta+\frac{1}{m}}) < \alpha$ for all $n \geq m$. Notice that the η -enlarged complement of $H_{-v,z}^{-1/m}$ is $\mathring{H}_{v,z}^{\eta+\frac{1}{m}}$. Furthermore $z \notin H_{-v,z}^{-1/m}$, hence there exists a direction $u = -v$ and a point $x = z - \frac{1}{m}v$ so that $z \notin H_{u,x}$ but $P(\mathring{H}_{-u,x}^\eta) < \alpha$. This last fact implies $z \notin \mathcal{H}_\alpha$, which is a contradiction. ■

Proof of Theorem 33. (i) and (ii) follow from point (i) of Theorem 32 and Zuo and Serfling [2000c, Theorem 3.1]; (iii) holds thanks to (iii) of Theorem 32; (iv) follows from points (iv) of Theorem 32 and Lemma 40. To prove point (v), we follow Rousseeuw and Ruts [1999, Proposition 1]. Let us fix $\alpha \geq 0$ and consider $x, y \in D_\alpha$. Given $0 < \gamma < 1$, let $z = \gamma x + (1 - \gamma)y$. Let us show that $d_\eta(z; P) \geq \min(d_\eta(x; P), d_\eta(y; P))$. For $u \in S^{p-1}$ there are two possibilities: (1) if $\langle u, y - x \rangle \geq 0$, we have that $H_{u,y}^\eta \subset H_{u,z}^\eta$; which implies $P(H_{u,z}^\eta) \geq P(H_{u,y}^\eta) \geq d_\eta(y; P)$; (2) if $\langle u, y - x \rangle < 0$, we have that $H_{u,x}^\eta \subset H_{u,z}^\eta$; which implies $P(H_{u,z}^\eta) \geq P(H_{u,x}^\eta) \geq d_\eta(x; P)$. ■

Proof of Corollary 34. This is a consequence of Theorem 33. For the proof see Rousseeuw and Ruts [1999, Proposition 7]. ■

Proof of Theorem 36.

$$\begin{aligned} \sup_{x \in \mathbb{R}^p} |d_{\eta,n}(x; P) - d_{\eta}(x; P)| &= \sup_{x \in \mathbb{R}^p} \left| \inf_{u \in S^{p-1}} P_n(H_{u,x}^{\eta}) - \inf_{u \in S^{p-1}} P(H_{u,x}^{\eta}) \right| \\ &\leq \sup_{x \in \mathbb{R}^p} \sup_{u \in S^{p-1}} |P_n(H_{u,x}^{\eta}) - P(H_{u,x}^{\eta})| \xrightarrow{n \rightarrow \infty} 0 \text{ a. s.} \end{aligned}$$

since the set of halfspaces is a Vapnik-Chervonenkis class [see, Burr and Fabrizio, 2016, and the references therein]. ■

Proof of Corollary 37. The η -halfspace depth vanishes at infinity and is upper semicontinuous because of Theorem 32. Moreover, the sample η -halfspace depth converges uniformly almost surely to its sample counterpart. Therefore, the proof is similar to that of Corollary 27. ■

6 Simulations

We consider four simulation settings, which include a missing data scenario and non-overlapping convex hulls scenario.

6.1 Overlapping convex-hulls

We provide three simulations under this scenario.

Simulation 1. When a supervised classifier is based on depth functions, it is well-known the problematic cause by the vanishing of the empirical depth outside the convex hull of the data: if a datum has depth zero when computed with respect to two distinct samples, it can not be clearly classify based on its depth value. The families of depth functions, and their corresponding sample versions, defined in this paper give a solution to this problem. Furthermore, the hypothesis required on the distribution for a good behavior of these families of depth functions are easily checked, as only a symmetry test is required [see, Ley and Paindaveine, 2011, and the references therein]. A prior solution for the sample depth was provided in Einmahl et al. [2015] for the particular case of the sample halfspace depth. The proposal was given under certain restrictive assumptions, which leave out the normal and uniform distribution among others. It has further disadvantages which include: (i) the non-affine invariance of the depth; (ii) the required hypothesis are not easy to be verified in practice; (iii) the need of selecting /estimating two constants; (iv) the performance for small sample sizes is not appropriate to have good estimations for the univariate projections and the probabilities in the tails; (v) the probability in the tails of unidimensional projections is estimated parametrically using the same function for every probability distribution.

Hereafter, we study empirically our proposal under the two-class classification scenario used in Einmahl et al. [2015, Section 3.2] to classify the elements with zero simplicial depth value with respect to two elliptical distributions that satisfy their assumptions on the distribution and two normal distributions; both cases under differences on location, scale and simultaneous location and scale

differences. For a more general classification algorithm see Cuesta-Albertos et al. [2017]. In Figure 3 we illustrate the obtained results for the sample simplex enlarged σ -simplicial depth for different values of σ , in the range from from 1.2 to 25, and for the sample simplicial depth ($\sigma = 1$). For details, see Table 1 in the Appendix, Section D. Comparing these results to the ones in Einmahl et al. [2015, Figure 7] it is evident that the misclassification rates obtained for the sample simplex enlarged σ -simplicial depth are dramatically lower in all the cases for quite moderate values of σ . A more extensive simulation study has

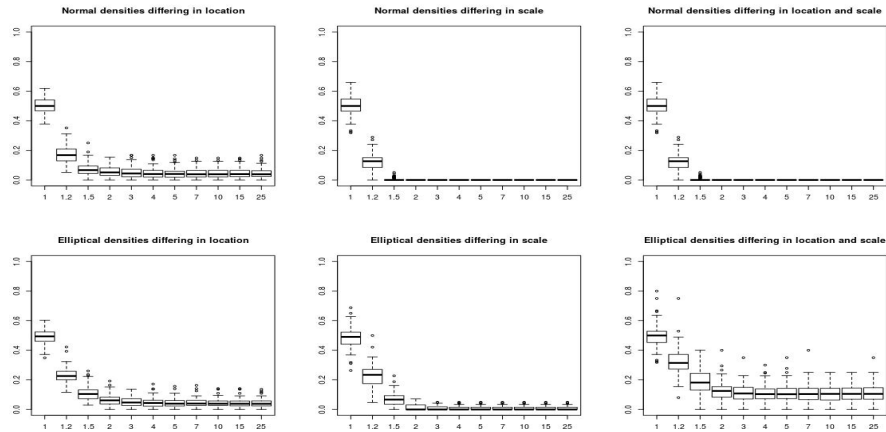


Figure 3: Boxplots of 100 misclassification rates of the points outside the data’s convex hull for $d_{\Delta,n}(\cdot, \cdot)$ with $\sigma \in \{1.2, 1.5, 2, 3, 4, 5, 7, 10, 15, 25\}$ and the sample simplicial depth ($\sigma = 1$). Linear DD-plot classifier.

been carried out and included in the Appendix, Section D. For instance, Table 2 includes the misclassification rates for all the elements in the sample. Figure 9 and Tables 3 and 4 repeat the study for the sample distribution enlarged σ -simplicial depth $d_{\sigma,k}(\cdot, \cdot)$ while Table 5 focuses on $d_{\sigma,n}(\cdot, \cdot)$. Figure 10 and Tables 6 and 7 redo it for the sample η -halfspace depth. The classifier used so far is a linear DD-classifier. To compare it with a more complex one, we have redone the study with a polynomial up to degree 10 DD-classifier for the sample simplex enlarged σ -simplicial depth (Figure 11 and Tables 8 and 9) and for the sample distribution enlarged σ -simplicial depth $d_{\sigma,k}(\cdot, \cdot)$ (Figure 12 and Tables 10 and 11).

Simulation 2. We perform a simulation under the scenario of four bivariate independent normal distributions with identity covariance matrix. We denote them by $P^{(1)}, P^{(2)}, P^{(3)}, P^{(4)}$. We take $P^{(1)}$ with mean $(-4, 0)$, $P^{(2)}$ with mean $(-\delta, 0)$ where $\delta \in (0, 4)$ and $P^{(4)}$ with mean $(4, 0)$. We consider two scenarios: (i) symmetric distributions: $P^{(3)}$ with mean $(\delta, 0)$; and (ii) asymmetric distributions: $P^{(3)}$ with mean $(2, 0)$. The perfect classifier would result on closeness of $P^{(2)}$ to $P^{(1)}$ and of $P^{(3)}$ to $P^{(4)}$.

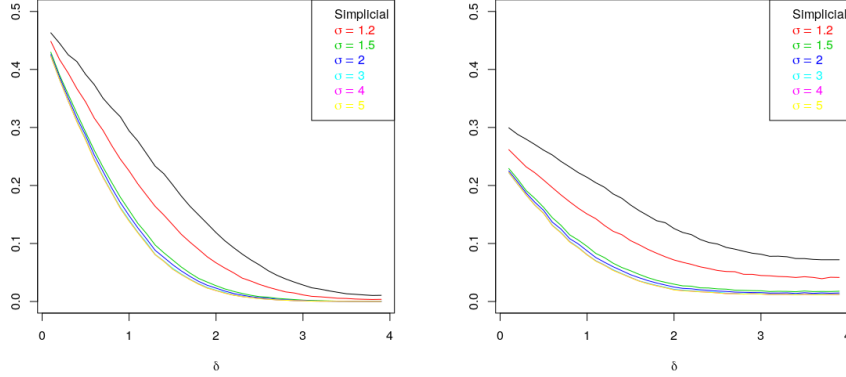


Figure 4: Mean, as a function of δ , of misclassification rates over 100 times using the sample simplicial depth and $d_{\Delta,n}(\cdot, \cdot)$ for $\sigma \in \{1.2, 1.5, 2, 3, 4, 5\}$. On the left symmetric distributions are given, on the right asymmetric ones.

We generate 500, training, samples from $P^{(1)}$ and another 500 from $P^{(4)}$ and 2500, test, samples from $P^{(2)}$ and another 2500 from $P^{(3)}$. The procedure is repeated 100 times for each $\delta \in \{.1, .2, .3, \dots, 3.9\}$. The mean of the misclassification rates using the sample simplicial depth and the sample simplex enlarged σ -simplicial depth for different values of σ are computed and plotted as a function of δ in Figure 4. Clearly, the sample simplex enlarged σ -simplicial depth outperforms the sample simplicial depth for all values of δ . Furthermore, the results are similar for any $\sigma \geq 1.5$, which shows that this procedure is stable with respect to the choice of σ .

Simulation 3. This is a simulation study where there are missing data. Let $P^{(1)}$ and $P^{(2)}$ be two bivariate independent normal distributions with identity covariance matrix; and respective means $(-2, 0)$ and $(2, 0)$. Let $\delta \in (0, 2)$. We consider two cases: (i) symmetric band: $\{(x, y) \in \mathbb{R}^2 : -\delta \leq x \leq \delta\}$ and (ii) asymmetric band: $\{(x, y) \in \mathbb{R}^2 : -\delta \leq x \leq 0\}$.

We draw 500, samples from $P^{(1)}$ and another 500 from $P^{(2)}$; and keep as training samples those that are outside the corresponding band. Then, we draw additional samples from $P^{(1)}$ and $P^{(2)}$ until there are 100 additional samples from each inside the band we are using. We keep these 200 samples as test samples. The maximum depth classifier is used to compute the mean of the misclassification rates over 100 times for each $\delta \in \{.05, .1, .15, \dots, 1.95\}$. Figure 5 displays the curves resulting of computing the sample simplicial and sample simplex enlarged σ -simplicial depth for $\sigma \in \{1, 1.2, 1.5, 2, 3, 4, 5\}$. Additionally, it displays the curve resulting of computing the sample simplicial depth with respect to all of the training samples; and not just the training samples outside the band as with the other seven curves.

In Figure 5, it happens that every curve takes a value approximately .5 when $\delta = .05$. Let us first study the symmetric case. In this case, this is due to we have an extremely narrow band and then, the distribution of the 100 elements of the test sample from $P^{(1)}$ has approximately the same amount of elements with the abscissa coordinate larger than zero than with it smaller than zero. The same occurs for $P^{(2)}$. Thus, the elements of the training sample are assigned indistinctly to either $P^{(1)}$ or $P^{(2)}$. This changes the moment that δ grows as it is more probable to find elements of the test sample that belongs to $P^{(1)}$ with $x < 0$. Analogously for $P^{(2)}$ with $x > 0$. The simplicial depth case is depicted in red. One can observe that, as delta grows, the misclassification rate decreases from the 50% as expected but it then increases back again. This is mainly due to three reasons: (i) The training sample size decreases as δ grows. (ii) For small values of δ it is expected to obtain samples drawn from $P^{(1)}$ on both regions of the complement of the band. However, as δ grows the probability of this happening rapidly decreases. (iii) When σ is small (1 for the simplicial depth) and δ is big, there are points in the band that have zero depth with respect to $P^{(1)}$ and with respect to $P^{(2)}$. Thus, they are assigned randomly. This characteristic of the simplicial depth is inherited by the σ -simplicial depth for small values of σ . However, for $\sigma \geq 3$ it is easily observed from the left plot in Figure 5, that our methodology is able to steadily overcome these issues. It is also important to notice the outstanding results as they are even better than computing the simplicial depth without missing data. The reason for this is that there are elements of the test sample that are outside the convex hull of $P^{(1)}$ and of $P^{(2)}$. This elements have zero simplicial depth but positive σ -simplicial depth if σ is not too small.

The asymmetric case is different, though. Let us first focus in the case of the simplicial depth without missing data. In this setting we have drawn training samples from two normal distributions that only differ in mean. The best separator of these two distributions is the line $x = 0$. The elements of the test sample (half from $P^{(1)}$ and half from $P^{(2)}$) have the x coordinate smaller or equal than 0 and, therefore, almost every element of the test sample is assigned to $P^{(1)}$, resulting in a misclassification rate close to .5, independently of δ . The missing data case works as follows. The training sample drawn from $P^{(1)}$ has a larger amount of elements with x coordinate larger than zero than the training sample drawn from $P^{(2)}$ has with x coordinate smaller than $-\delta$. Thus, as before, the simplicial depth assigns most of the elements in the test sample to $P^{(1)}$. Similarly occurs for the σ -simplicial depth for small values of σ . When σ increases, the σ -simplicial depth overcomes this issue because the amount of simplices covering the band increases rapidly. The reason for every curve taking a value approximately .5 when $\delta = .05$, is similar to that of the symmetric case, as there is an extremely narrow band.

6.2 Non-overlapping convex-hulls

Simulation 4. We perform a simulation under the simple scenario of four independent uniform distributions over the intervals $[-2, -1]$, $(-1, 0)$, $(0, 1)$ and

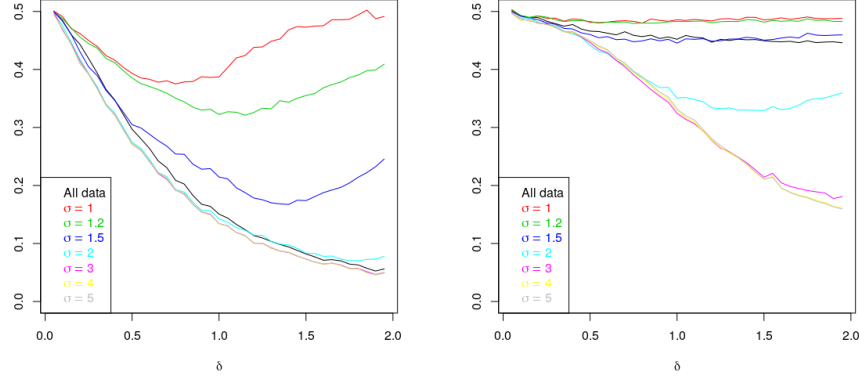


Figure 5: Mean, as a function of δ , of misclassification rates over 100 times using the sample simplicial depth and $d_{\Delta,n}(\cdot, \cdot)$ for $\sigma \in \{1, 1.2, 1.5, 2, 3, 4, 5\}$. Symmetric band (left) and asymmetric band (right).

[1, 2]. We denote them by $P^{(1)}, P^{(2)}, P^{(3)}$ and $P^{(4)}$, respectively. In this experiment, we consider two sample sizes $n = 100, 1000$ for the random draws from $P^{(1)}$ and $P^{(4)}$. We use them to assign each of 2500 observations generated from $P^{(2)}$ and 2500 from $P^{(3)}$ to either the group defined by $P^{(1)}$ or $P^{(4)}$. Note that the perfect assignment would allocate closeness to $P^{(1)}$ to each of the observations from $P^{(2)}$ and to $P^{(4)}$ to each of the observations from $P^{(3)}$. The assignment can be performed using any of the depth functions we have proposed in this paper together with a depth based classifier. To exemplify it, we make use of the proposed sample version of the simplex enlarged σ -simplicial depth and the maximum depth classifier. Although more complex classifiers exist in the literature, the maximum depth classifier suffices to show the outperformance of the enlarged depth over the classical.

In Figure 6 we show the median (solid line), the 25% and 75% quantiles (dashed lines) and the whiskers of the boxplot (dotted lines) of the misclassification rates when the procedure is repeated 1000 times for different values of σ . The value $\sigma = 1$ is the case of the sample simplicial depth which has about 50 percent of misclassification rate. The misclassification rates of the sample simplex enlarged σ -simplicial depth rapidly decreases. For extremely large values of σ , the misclassification rate increases due to every enlarged simplex contains each of the points we aim to classify. The optimal sample value of σ as displayed in the figure is obtained around 3.28 for $n = 100$ and around 3.02 for $n = 1000$. We elaborate on this in the next section.

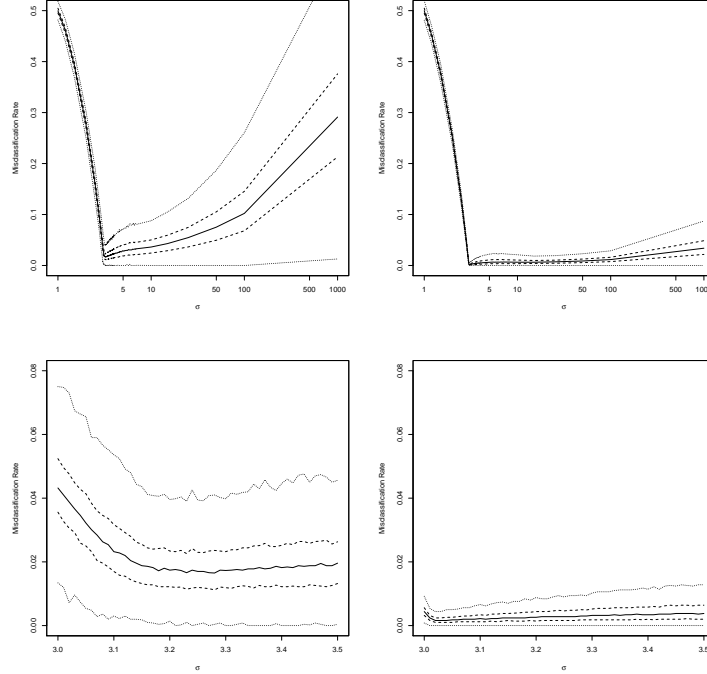


Figure 6: Median (solid line), 25% and 75% quantiles (dashed lines) and whiskers of the boxplot (dotted lines) of the misclassification rates for different values of σ , sample sizes $n = 100$ (left plots) and $n = 1000$ (right plots). The bottom plots are a zoomed version of the above plots.

7 Future work

As studied in the paper, the theoretical properties for the σ -simplicial depth functions are satisfied for any sigma. However, the choice of σ is relevant for applications. For instance, let $P^{(1)}$ and $P^{(2)}$ be two independent uniform distributions over the intervals $[-2, -1]$ and $[1, 2]$. Assume the objective is to assign the points in the interval $(-1, 0)$ to $P^{(1)}$ and those in the interval $(0, 1)$ to $P^{(2)}$. A perfect classifier would be given by using a σ such that the depth with respect to $P^{(1)}$ is positive for any point in $(-1, 0)$ and zero for any in $(0, 1)$; and, analogously, the depth with respect to $P^{(2)}$ is positive for any point in $(0, 1)$ and zero for any in $(-1, 0)$. If we make use of either the distribution or simplex enlarged σ -simplicial depth for this task, the appropriate sigma is $\sigma = 3$. For the distribution enlarged σ -simplicial depth, the reason is that $d_\sigma(x, P)$ is equal to the simplicial depth with respect P_σ and the support of $P_3^{(1)}$ is the interval $[-3, 0]$ while the support of $P_3^{(2)}$ is the interval $[0, 3]$. Larger values of

σ provide larger supports while smaller values of σ provide shorter supports. For the simplex enlarged σ -simplicial depth notice that for $\sigma = 3$ the largest enlarged simplex of elements from $P^{(1)}$ is the interval $[-3, 0]$; and equivalently for $P^{(2)}$. Thus, future work will be dedicated to the study of the estimation of the appropriate σ under different applications. For example, the estimation of sigma in Simulation 4 for optimality of the classification rate.

A Counterexamples for Section 2

Propositions 2 and 3 do not apply for neither angular nor halfspace symmetry, as we show in the following counterexamples. These counterexamples picture random variables that are angular, and consequently halfspace, symmetric but that are not central symmetric. Counterexample 41 provides a distribution on \mathbb{R} , where the notion of symmetric distribution is unique and coincide with that of spherical, elliptical and central symmetry. On \mathbb{R} , all distributions are angular and halfspace symmetric about the distribution median. Thus, in this counterexample, the affine combination is still angular and halfspace symmetric but the center of symmetry differs from the one stated in the above two propositions.

Counterexample 41 *Let X_1, X_2 be two independent and identically distributed random variables on \mathbb{R} with the exponential distribution of parameter 1, which is symmetric about $\log(2)$ with respect to angular and halfspace symmetry. $X_1 + X_2$ follows a gamma distribution of parameters $(2, 1)$, which is also symmetric with respect to these two notions. If Proposition 2 were to be satisfied, the center of symmetry of the distribution associated to $X_1 + X_2$ would be $2\log(2)$; however, the center of angular and halfspace symmetry is the median of this gamma distribution, which is the solution of $(m + 1)e^{-m} = .5$, 1.39 approximately.*

The below counterexamples consider distributions on \mathbb{R}^2 . In each of them, the affine combination of two angular, and halfspace, symmetric distributions is neither angular, nor halfspace symmetric. Counterexamples 42 and 43 concern discrete distributions; there is no mass on the center of symmetry in the first one but there is in the second.

Counterexample 42 *Let X_1, X_2 be two independent and identically distributed random variables on \mathbb{R}^2 with the discrete uniform distribution on the set $\{(-1, 0), (-1, -1), (3, 0), (3, 3)\}$. This distribution is angular, and halfspace, symmetric about $(0, 0)$ but the distribution associated to the random variable $X_1 + X_2$ is neither angular nor halfspace symmetric.*

We have that $\mathbb{P}_{X_1+X_2}(-2, -2) = \mathbb{P}_{X_1+X_2}(-2, 0) = \mathbb{P}_{X_1+X_2}(6, 0) = \mathbb{P}_{X_1+X_2}(6, 6) = 1/16$ and $\mathbb{P}_{X_1+X_2}(-2, -1) = \mathbb{P}_{X_1+X_2}(2, -1) = \mathbb{P}_{X_1+X_2}(2, 0) = \mathbb{P}_{X_1+X_2}(2, 2) = \mathbb{P}_{X_1+X_2}(2, 3) = \mathbb{P}_{X_1+X_2}(6, 3) = 1/8$. Selecting the lines $y = 0$ and $x = 2$, we obtain that $(2, 0)$ is the only possible center of symmetry. However, it is easy to see that it is not the case by considering for instance the line $y = x - 2$.

Counterexample 43 Let X_1, X_2 be two independent and identically distributed random variables on \mathbb{R}^2 with the discrete uniform distribution on the set $\{(0, 0), (-1, 0), (-2, -2), (3, 0), (4, 4)\}$. This distribution is angular, and halfspace, symmetric about $(0, 0)$ but the distribution associated to the random variable $X_1 + X_2$ is neither angular nor halfspace symmetric.

It suffices to notice that $\mathbb{P}_{X_1+X_2}(0, 0) = \mathbb{P}_{X_1+X_2}(-2, 0) = \mathbb{P}_{X_1+X_2}(-4, -4) = \mathbb{P}_{X_1+X_2}(6, 0) = \mathbb{P}_{X_1+X_2}(8, 8) = 1/25$ and $\mathbb{P}_{X_1+X_2}(-1, 0) = \mathbb{P}_{X_1+X_2}(-2, -2) = \mathbb{P}_{X_1+X_2}(3, 0) = \mathbb{P}_{X_1+X_2}(4, 4) = \mathbb{P}_{X_1+X_2}(-3, -2) = \mathbb{P}_{X_1+X_2}(2, 0) = \mathbb{P}_{X_1+X_2}(3, 4) = \mathbb{P}_{X_1+X_2}(1, -2) = \mathbb{P}_{X_1+X_2}(2, 2) = \mathbb{P}_{X_1+X_2}(7, 4)$ and consider the same lines than in the previous counterexample.

The next paragraphs contain two counterexamples where the involved random variables are continuous. The first one is a modification of Counterexample 42: the distribution is concentrated on open balls instead of discrete points. The support of the random variables involved in the second is, however, the entire \mathbb{R}^2 .

Counterexample 44 Given $\epsilon \in (0, 1/8)$, let X_1, X_2 be two independent and identically distributed random variables on \mathbb{R}^2 with density function

$$f(x, y) = \frac{1}{4} \frac{1}{\pi \epsilon^2} \left[\mathbf{I}_{B_{(-1,0)}^\epsilon}(x, y) + \mathbf{I}_{B_{(-1,-1)}^\epsilon}(x, y) + \frac{1}{9} \left(\mathbf{I}_{B_{(3,0)}^{3\epsilon}}(x, y) + \mathbf{I}_{B_{(3,3)}^{3\epsilon}}(x, y) \right) \right],$$

where $B_{(a,b)}^\epsilon$ denotes the open ball with center (a, b) and radius ϵ . Then, taking into account that the Minkowski sum of $B_{(a_1,b_1)}^{r_1}$ and $B_{(a_2,b_2)}^{r_2}$ is $B_{(a_1+a_2,b_1+b_2)}^{r_1+r_2}$, it is obtained that $X_1 + X_2$ has probability mass $1/16$ in each of the open balls $B_{(-2,0)}^{2\epsilon}$, $B_{(-2,-2)}^{2\epsilon}$, $B_{(6,0)}^{6\epsilon}$, $B_{(6,6)}^{6\epsilon}$, and $1/8$ in $B_{(-2,-1)}^{2\epsilon}$, $B_{(2,-1)}^{4\epsilon}$, $B_{(2,0)}^{4\epsilon}$, $B_{(2,2)}^{4\epsilon}$, $B_{(2,3)}^{4\epsilon}$ and $B_{(6,3)}^{6\epsilon}$. It follows that $X_1 + X_2$ is not halfspace, nor angular, symmetric. If $X_1 + X_2$ were to be symmetric, its center would belong to the rectangle $R_\epsilon := \{(x, y) \in \mathbb{R}^2 : 2 - 4\epsilon \leq x \leq 2 + 4\epsilon, -6\epsilon \leq y \leq 6\epsilon\}$, but considering, for instance, the line $y = 73/80x - 9/16$, we reach a contradiction. See the left plot of Figure 7 for an illustration.

Counterexample 45 Let X_1, X_2 be two independent random variables on \mathbb{R}^2 whose distribution is a mixture of four bivariate normal distributions with equal weights, respective means $\mu_1 = (-1, 0)$, $\mu_2 = (-1, -1)$, $\mu_3 = (3, 0)$ and $\mu_4 = (3, 3)$ and covariance matrices $\Sigma_1 = \Sigma_2 = \sigma^2 I$ and $\Sigma_3 = \Sigma_4 = 9\sigma^2 I$ for some $\sigma > 0$. It is not difficult to see that this distribution is angular, and halfspace, symmetric about $(0, 0)$, while $X_1 + X_2$ is neither angular nor halfspace symmetric.

Note that $X_1 + X_2$ is a mixture of ten normal distribution with respective weights $\omega_1 = \omega_2 = \omega_3 = \omega_4 = \frac{1}{16}$ and $\omega_5 = \omega_6 = \omega_7 = \omega_8 = \omega_9 = \omega_{10} = \frac{1}{8}$, means $\mu_1 = (-2, 0)$, $\mu_2 = (-2, -2)$, $\mu_3 = (6, 0)$, $\mu_4 = (6, 6)$, $\mu_5 = (-2, -1)$, $\mu_6 = (2, -1)$, $\mu_7 = (2, 0)$, $\mu_8 = (2, 2)$, $\mu_9 = (2, 3)$ and $\mu_{10} = (6, 3)$ and covariance matrices $\Sigma_i = c\sigma^2 I$ with $c = 2$ for $i \in \{1, 2, 5\}$, $c = 18$ for $i \in \{3, 4, 10\}$

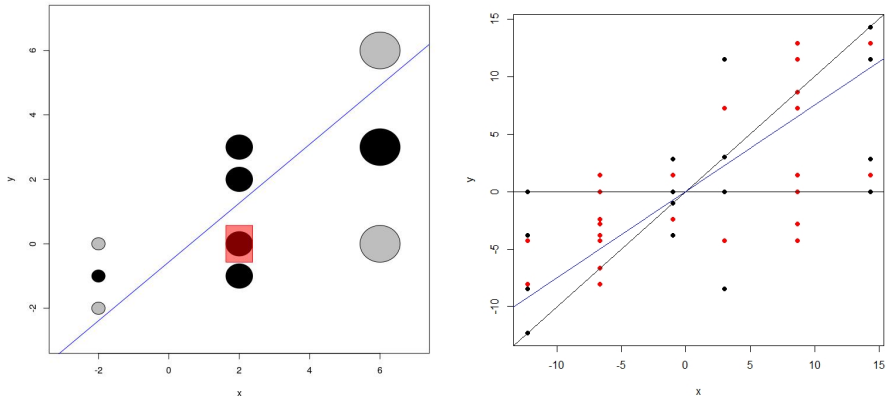


Figure 7: Left: For $\epsilon = 0.095$, in black the discs with mass $1/8$, in grey the discs with mass $1/16$ and in red the rectangle R_ϵ . The line $y = 73/80x - 9/16$ is plotted in blue. Right: The support of the random variable $(1 + 2\lambda)X_1 - \lambda X_2 - \lambda X_3$ for $\lambda = \sqrt{2}$. The black points have mass $1/64$, the red points $1/32$.

and $c = 10$ for $i \in \{6, \dots, 9\}$. In order to see that X_1, X_2 are angular symmetric about 0, it is enough to consider all the straight lines through the origin and see that the corresponding halfspaces have probability $1/2$. To prove that $X_1 + X_2$ is not angularly symmetric, we restrict ourselves to a single possible candidate for center of symmetry by considering the straight lines parallel to the axes and taking the two lines whose corresponding halfspaces have probability $1/2$. Then, it suffices to observe that there exists another straight line that passes through this point but which does not provide mass $1/2$ to its corresponding halfspaces. Therefore, there is no center of symmetry. For simplicity all this computations were done numerically.

The next counterexample is a modification of Counterexample 42 to include the type of affine combinations on which we focus in Section 3, and for which we study the symmetry under affine combinations on this section. For a continuous version of this counterexample, just replace, as in Counterexample 44, the points in the support by uniformly distributed open balls with center on these points, or consider, for instance, a mixture of normal distributions with mean on these points, as in Counterexample 45.

Counterexample 46 Let X_1, X_2, X_3 be three independent and identically distributed random variables on \mathbb{R}^2 following the distribution given in Counterexample 42. Then, for any $\lambda \neq 0$, the distribution of $(1 + 2\lambda)X_1 - \lambda X_2 - \lambda X_3$ is neither halfspace, nor angular symmetric. The reasoning for that is equivalent to the one provided in Counterexample 42. We illustrate it in the right plot of Figure 7, where any of the halfspaces that has a black line as border have at least

probability mass $1/2$ while one of the halfspaces with the blue line as border has smaller probability mass: the one containing the point $(5, 0)$.

The next counterexample applies only to Proposition 3, as in this counterexample the random variables are not identically distributed.

Counterexample 47 Let X_1, X_2 be two independent random variables on \mathbb{R}^2 with the following distributions: $\mathbb{P}_{X_1}(0, 0) = \mathbb{P}_{X_2}(0, 0) = 1/5$, $\mathbb{P}_{X_1}(-1, 0) = \mathbb{P}_{X_1}(5, 0) = 2/5$ and $\mathbb{P}_{X_2}(0, 3) = \mathbb{P}_{X_2}(0, -7) = 2/5$. X_1 and X_2 are both angular, and halfspace, symmetric about $(0, 0)$; but $X_1 + X_2$ is neither angular nor halfspace symmetric.

Let us see that $X_1 + X_2$ is not halfspace symmetric, and consequently not angularly symmetric. Denoting $Y := X_1 + X_2$, we have that $\mathbb{P}_Y(-1, 3) = \mathbb{P}_Y(4, 0) = \mathbb{P}_Y(0, -4) = \mathbb{P}_Y(5, -7) = 4/25$, $\mathbb{P}_Y(-1, 0) = \mathbb{P}_Y(0, 3) = \mathbb{P}_Y(0, -7) = \mathbb{P}_Y(5, 0) = 2/25$ and $\mathbb{P}_Y(0, 0) = 1/25$. Considering the halfspaces in which the plane is divided by the coordinate axes, it is easy to see that the origin is the only possible center of symmetry. However, the upper halfspace determined by any other straight line in the first and third quadrant through the origin has mass smaller than $1/2$.

B Counterexample for Section 3

Here it is shown that, in general, the simplex enlarged σ -simplicial depth does not satisfy the maximality at the center property for spherically symmetric distributions; and that it is not monotonically decreasing from the center of symmetry.

Let $p = 1$ and $\sigma > 1$. As in the proof of Proposition 16, the simplex enlarged σ -simplicial depth of $x \in \mathbb{R}$ is given by

$$d_{\Delta}(x; P) = \int_{S^+(x)} dP(x_1)dP(x_2) + \int_{S^-(x)} dP(x_1)dP(x_2) - \int_{\{(x,x)\}} dP(x_1)dP(x_2)$$

where the sets

$$S^+(x) := \left\{ (x_1, x_2) \in \mathbb{R}^2 : \frac{1+\sigma}{2}x_1 + \frac{1-\sigma}{2}x_2 \leq x \leq \frac{1-\sigma}{2}x_1 + \frac{1+\sigma}{2}x_2 \right\}$$

$$S^-(x) := \left\{ (x_1, x_2) \in \mathbb{R}^2 : \frac{1-\sigma}{2}x_1 + \frac{1+\sigma}{2}x_2 \leq x \leq \frac{1+\sigma}{2}x_1 + \frac{1-\sigma}{2}x_2 \right\}$$

have only the point (x, x) in common. For $c > 0$ and $0 < \epsilon \leq \min(\sigma - 1, 2)c/\sigma$, let us consider the probability distribution P with density function given by

$$f(x) = \frac{1}{4\epsilon} [\mathbf{I}_{(-\epsilon-c, -c+\epsilon)}(x) + \mathbf{I}_{(-\epsilon+c, c+\epsilon)}(x)]. \quad (4)$$

Clearly, P is symmetric about 0. Note that $S := (-\epsilon - c, -c + \epsilon) \cup (-\epsilon + c, c + \epsilon)$ is the support of f and that $S \times S = S_{++} \cup S_{+-} \cup S_{-+} \cup S_{--}$, with $S_{++} :=$

$(-\epsilon + c, c + \epsilon) \times (-\epsilon + c, c + \epsilon)$, $S_{+-} := (-\epsilon + c, c + \epsilon) \times (-\epsilon - c, -c + \epsilon)$, $S_{-+} := (-\epsilon - c, -c + \epsilon) \times (-\epsilon + c, c + \epsilon)$ and $S_{--} := (-\epsilon - c, -c + \epsilon) \times (-\epsilon - c, -c + \epsilon)$ disjoint sets. Then, the simplex enlarged σ -simplicial depth of x is

$$\begin{aligned} d_{\Delta}(x; P) &= \int_{S^+(x)} f(x_1)f(x_2) dx_1 dx_2 + \int_{S^-(x)} f(x_1)f(x_2) dx_1 dx_2 \\ &= \frac{1}{4\epsilon} \lambda(S^+(x) \cap (S_{++} \cup S_{+-} \cup S_{-+} \cup S_{--})) \\ &\quad + \frac{1}{4\epsilon} \lambda(S^-(x) \cap (S_{++} \cup S_{+-} \cup S_{-+} \cup S_{--})) \end{aligned}$$

where λ denotes the Lebesgue measure. For $0 \leq \alpha < 1$ we compare the depth difference of the points αc and c , $d_{\Delta}(\alpha c; P) - d_{\Delta}(c; P)$. Since $\epsilon \leq (\sigma - 1)/\sigma c$ we have that S_{-+} is a subset of both $S^+(c)$ and $S^+(\alpha c)$, and that S_{+-} is a subset of both $S^-(c)$ and $S^-(\alpha c)$. On the contrary, since $\epsilon \leq 2/\sigma c$, S_{--} does not belong to any of the sets $S^+(c)$, $S^-(c)$, $S^+(\alpha c)$ and $S^-(\alpha c)$. It follows that

$$\begin{aligned} d_{\Delta}(\alpha c; P) - d_{\Delta}(c; P) &= \\ &= \frac{1}{4\epsilon} (\lambda((S^+(\alpha c) \cup S^-(\alpha c)) \cap S_{++}) - \lambda((S^+(c) \cup S^-(c)) \cap S_{++})), \end{aligned}$$

which is smaller than 0. Thus, the simplex enlarged σ -simplicial depth is not monotonically decreasing from 0. This is illustrated in Figure 8.

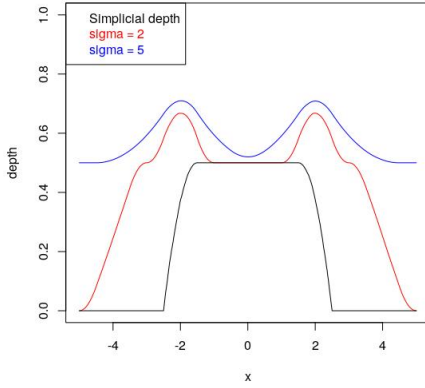


Figure 8: The sample simplicial and simplex enlarged σ -simplicial depth for $\sigma \in \{2, 5\}$ of the distribution P with density (4) for $c = 2$ and $\epsilon = 0.5$; constructed with 10^4 samples drawn from P .

C Definition

The expression of $d_{\sigma,n}$ in Definition 23 involves more summation terms than required; for ease of understanding. The statement below does not involve unnecessary terms.

Let P be a given distribution on \mathbb{R}^{p-1} , $\sigma > 1$, $n \geq p^2$ and P_n the empirical distribution associated to a sample X_1, \dots, X_n of random draws taken from P . Then, for any $x \in \mathbb{R}^{p-1}$,

$$d_{\sigma,n}(x, P) = a \sum_{\substack{1 \leq i_1 < \dots < i_p \leq n \\ \{j_{1,1}, \dots, j_{1,p-1}\}, \dots, \\ \{j_{p,1}, \dots, j_{p,p-1}\} \\ \subset \{1, \dots, n\} \\ \text{all indexes differ}}} \mathbf{I}(x \in \Delta[Y_{i_1, j_{1,1}}, \dots, j_{1,p-1}}, \dots, Y_{i_p, j_{p,1}}, \dots, j_{p,p-1}}]),$$

where $a := \frac{(n-p^2)! p! ((p-1)!)^p}{n!}$.

The summation above is over all possible choices of the X 's that give rise to different simplices. It is obtained as follows.

1. Choose p^2 among n random draws to be the ones exploited for computing the vertices of the simplex. There are $\binom{n}{p^2}$ ways to do this.
2. Choose p among the p^2 random draws to be the X_{i_k} $k = 1, \dots, p$ which have coefficient $\sigma + \frac{1-\sigma}{p}$. There are $\binom{p^2}{p}$ ways to do this.
3. Split the remaining $p(p-1)$ random draws into p groups of size $p-1$. That is, the groups $\{X_{j_{k,1}}, \dots, X_{j_{k,p-1}}\}$ associated with X_{i_k} for $k = 1, \dots, p$. There are $\frac{(p^2-p)!}{((p-1)!)^p}$ ways to do this.

All together, we obtain $\binom{n}{p^2} \binom{p^2}{p} \frac{(p^2-p)!}{((p-1)!)^p} = \frac{n!}{(n-p^2)! p! ((p-1)!)^p}$.

D Further simulations

Table 1 shows the results when we classify only the points outside the convex hull of the data sample, obviously the results are much better for the sample simplex enlarged σ -simplicial depth than for the sample simplicial depth since in this last case points are assigned randomly. The performance of our procedure is still better even when we classify the whole sample as it is shown in Table 2. Comparing Table 1 with Table 3 (see also Figure 3 in the main paper and Figure 9 here) it is clear that $d_{\Delta,n}$ performs much better than $d_{\sigma,k(n,p)}$. Moreover the choice of σ is more relevant for $d_{\sigma,k(n,p)}$. The gap is smaller, however, for the whole sample case as it can be seen by comparing Table 2 with Table 4. Therefore $d_{\sigma,k(n,p)}$ is a good contender for large amounts of data due to its efficiency. The results of Table 5 for $d_{\sigma,n}$ are similar to what it happens in Tables 1 and 2 for $d_{\Delta,n}$. Tables 6 and 7 refer to the enlarged η -halfspace depth, comparing those results with the obtained by Einmahl et al. [2015] our procedure

is performing better or equivalently. Tables 8, 9, 10 and 11 use up to degree 10 polynomial classifier as implemented in the `ddalpha` R package [Pokotylo et al., 2016]. The results are similar to those using the linear classifier.

Misclassification rates for the points outside the convex hulls						
	Bivariate normal			Bivariate elliptical		
	location	scale	location & scale	location	scale	location & scale
simplicial	0.50533 (0.05674)	0.50276 (0.06706)	0.50276 (0.06706)	0.49118 (0.04874)	0.48744 (0.07265)	0.49464 (0.07598)
$\sigma = 1.2$	0.17180 (0.05935)	0.12619 (0.05360)	0.12619 (0.05360)	0.22805 (0.05120)	0.22485 (0.07430)	0.31783 (0.09219)
$\sigma = 1.5$	0.07402 (0.04288)	0.00479 (0.00977)	0.00495 (0.0101)	0.10800 (0.04600)	0.06691 (0.04633)	0.18556 (0.07938)
$\sigma = 2$	0.05783 (0.03698)	0 (0)	0 (0)	0.06585 (0.03707)	0.01636 (0.01984)	0.12264 (0.06152)
$\sigma = 3$	0.04994 (0.03815)	0 (0)	0 (0)	0.05163 (0.03031)	0.00773 (0.01243)	0.11572 (0.05851)
$\sigma = 4$	0.04662 (0.03616)	0 (0)	0 (0)	0.04521 (0.03061)	0.00738 (0.01226)	0.10894 (0.05684)
$\sigma = 5$	0.04524 (0.03509)	0 (0)	0 (0)	0.04349 (0.02789)	0.00665 (0.01149)	0.11050 (0.05840)
$\sigma = 7$	0.04445 (0.03410)	0 (0)	0 (0)	0.04544 (0.02860)	0.00652 (0.01150)	0.10929 (0.06112)
$\sigma = 10$	0.04446 (0.03295)	0 (0)	0 (0)	0.04432 (0.02759)	0.00652 (0.01150)	0.10634 (0.05280)
$\sigma = 15$	0.04522 (0.03342)	0 (0)	0 (0)	0.04368 (0.02770)	0.00652 (0.01150)	0.10881 (0.05427)
$\sigma = 25$	0.04533 (0.03388)	0 (0)	0 (0)	0.04298 (0.02678)	0.00652 (0.01150)	0.11004 (0.05830)
$\sigma = 50$	0.04462 (0.03384)	0 (0)	0 (0)	0.04412 (0.02682)	0.00652 (0.01150)	0.10720 (0.05221)
$\sigma = 10^2$	0.04431 (0.03386)	0 (0)	0 (0)	0.04451 (0.02696)	0.00652 (0.01150)	0.10740 (0.05188)
$\sigma = 10^3$	0.04522 (0.03452)	0 (0)	0 (0)	0.04334 (0.02687)	0.00652 (0.01150)	0.10793 (0.05526)
$\sigma = 10^4$	0.04504 (0.03297)	0 (0)	0 (0)	0.04399 (0.02671)	0.00652 (0.01150)	0.10983 (0.05856)
$\sigma = 10^5$	0.04599 (0.03366)	0 (0)	0 (0)	0.04477 (0.02762)	0.00652 (0.01150)	0.10675 (0.05539)

Table 1: Mean and standard deviation, in parenthesis, of 100 misclassification rates of the points outside the data convex hull for $d_{\Delta,n}(\cdot, \cdot)$ with $\sigma \in \{1.2, 1.5, 2, 3, 4, 5, 7, 10, 15, 25, 50, 10^2, 10^3, 10^4, 10^5\}$ and the sample simplicial depth ($\sigma = 1$). Linear DD-plot classifier.

Misclassification rates						
	Bivariate normal			Bivariate elliptical		
	location	scale	location & scale	location	scale	location & scale
simplicial	0.08793 (0.00488)	0.17455 (0.00655)	0.12963 (0.00614)	0.00864 (0.00259)	0.16003 (0.00788)	0.03593 (0.00443)
$\sigma = 1.2$	0.08364 (0.00420)	0.16866 (0.00581)	0.12540 (0.00510)	0.00415 (0.00124)	0.15279 (0.00629)	0.03145 (0.00386)
$\sigma = 1.5$	0.08140 (0.00405)	0.16622 (0.00648)	0.12286 (0.00511)	0.00221 (0.00086)	0.14589 (0.00549)	0.02824 (0.00307)
$\sigma = 2$	0.08074 (0.00408)	0.16542 (0.00637)	0.12136 (0.00520)	0.00154 (0.00085)	0.14419 (0.00520)	0.02639 (0.00277)
$\sigma = 3$	0.08060 (0.00429)	0.16520 (0.00632)	0.12143 (0.00546)	0.00122 (0.00063)	0.14517 (0.00548)	0.02606 (0.00286)
$\sigma = 4$	0.0807 (0.00429)	0.16488 (0.00606)	0.12117 (0.00534)	0.0011 (0.00058)	0.14634 (0.00556)	0.02605 (0.00252)
$\sigma = 5$	0.08061 (0.00439)	0.16511 (0.00677)	0.12130 (0.00554)	0.00109 (0.00058)	0.14688 (0.00609)	0.02617 (0.00268)
$\sigma = 7$	0.08062 (0.00430)	0.16498 (0.00581)	0.12130 (0.00522)	0.00111 (0.00060)	0.14669 (0.00575)	0.02613 (0.00278)
$\sigma = 10$	0.08031 (0.00413)	0.16529 (0.00654)	0.12158 (0.00538)	0.00109 (0.00059)	0.14654 (0.00571)	0.02614 (0.00269)
$\sigma = 15$	0.08044 (0.00414)	0.16502 (0.00595)	0.12210 (0.00521)	0.00107 (0.00059)	0.14668 (0.00582)	0.02624 (0.00271)
$\sigma = 25$	0.08037 (0.00407)	0.16529 (0.00611)	0.12303 (0.00545)	0.00106 (0.00057)	0.14655 (0.00589)	0.02626 (0.00272)
$\sigma = 50$	0.08037 (0.00402)	0.16531 (0.00603)	0.12336 (0.00524)	0.00108 (0.00058)	0.14658 (0.00576)	0.02608 (0.00260)
$\sigma = 10^2$	0.08039 (0.00404)	0.16539 (0.00612)	0.12358 (0.00524)	0.00110 (0.00058)	0.14671 (0.00569)	0.02607 (0.00263)
$\sigma = 10^3$	0.08024 (0.00401)	0.16512 (0.00610)	0.12377 (0.00495)	0.00108 (0.00057)	0.14686 (0.00593)	0.02620 (0.00284)
$\sigma = 10^4$	0.08063 (0.00408)	0.16554 (0.00658)	0.12345 (0.00506)	0.00109 (0.00057)	0.14677 (0.00583)	0.02622 (0.00287)
$\sigma = 10^5$	0.08070 (0.00399)	0.16556 (0.00632)	0.12361 (0.00528)	0.00108 (0.00059)	0.14737 (0.00612)	0.02632 (0.00270)

Table 2: Mean and standard deviation, in parenthesis, of 100 misclassification rates, using the whole sample, for $d_{\Delta,n}(\cdot, \cdot)$ with $\sigma \in \{1.2, 1.5, 2, 3, 4, 5, 7, 10, 15, 25, 50, 10^2, 10^3, 10^4, 10^5\}$ and the sample simplicial depth ($\sigma = 1$). Linear DD-plot classifier.

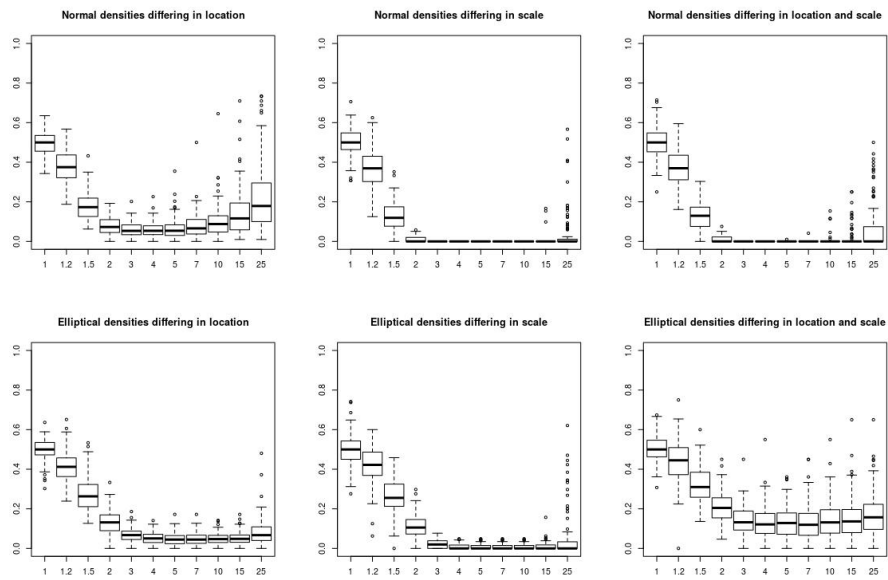


Figure 9: Boxplots of 100 misclassification rates of the points outside the data convex hull for $d_{\sigma,k}(\cdot, \cdot)$ with $\sigma \in \{1.2, 1.5, 2, 3, 4, 5, 7, 10, 15, 25\}$ and the sample simplicial depth ($\sigma = 1$). Linear DD-plot classifier.

Misclassification rates for the points outside the convex hulls						
	Bivariate normal			Bivariate elliptical		
	location	scale	location & scale	location	scale	location & scale
$\sigma = 1$	0.49753 (0.05921)	0.50182 (0.07334)	0.50557 (0.07644)	0.49722 (0.0553)	0.50059 (0.0786)	0.50459 (0.06559)
$\sigma = 1.2$	0.3764 (0.0809)	0.36528 (0.09222)	0.37282 (0.08744)	0.41504 (0.07598)	0.42165 (0.10046)	0.43982 (0.10106)
$\sigma = 1.5$	0.17484 (0.06557)	0.12956 (0.06994)	0.1298 (0.06798)	0.2728 (0.08405)	0.26422 (0.08302)	0.32288 (0.08739)
$\sigma = 2$	0.07713 (0.04234)	0.01018 (0.01439)	0.0109 (0.01528)	0.13493 (0.05794)	0.11319 (0.05807)	0.21014 (0.08081)
$\sigma = 3$	0.05947 (0.03715)	0 (0)	0 (0)	0.0688 (0.03318)	0.02274 (0.02333)	0.14457 (0.07135)
$\sigma = 4$	0.06118 (0.04048)	0 (0)	0 (0)	0.05339 (0.02813)	0.00851 (0.01347)	0.1291 (0.07909)
$\sigma = 5$	0.06768 (0.05468)	0 (0)	0.0001 (0.00103)	0.04631 (0.02915)	0.00705 (0.01199)	0.1321 (0.07873)
$\sigma = 7$	0.079 (0.06667)	0 (0)	0.00041 (0.0041)	0.04716 (0.02968)	0.00686 (0.01195)	0.13274 (0.0861)
$\sigma = 10$	0.10207 (0.0857)	0 (0)	0.00463 (0.02251)	0.05024 (0.02914)	0.00686 (0.01195)	0.14471 (0.09359)
$\sigma = 15$	0.14756 (0.12308)	0.00419 (0.02437)	0.01745 (0.04901)	0.0533 (0.0325)	0.00972 (0.0202)	0.1558 (0.10879)
$\sigma = 25$	0.22551 (0.17965)	0.04055 (0.10403)	0.06976 (0.12466)	0.08301 (0.07041)	0.05845 (0.12371)	0.17382 (0.11458)

Table 3: Mean and standard deviation, in parenthesis, of 100 misclassification rates of the points outside the data convex hull for $d_{\sigma,k}(\cdot, \cdot)$ with $\sigma \in \{1.2, 1.5, 2, 3, 4, 5, 7, 10, 15, 25\}$ and the sample simplicial depth ($\sigma = 1$). Linear DD-plot classifier.

Misclassification rates						
	Bivariate normal			Bivariate elliptical		
	location	scale	location & scale	location	scale	location & scale
$\sigma = 1$	0.09976 (0.00617)	0.19473 (0.0118)	0.14565 (0.00931)	0.02407 (0.00757)	0.1825 (0.01562)	0.04707 (0.0076)
$\sigma = 1.2$	0.09008 (0.00514)	0.17944 (0.00848)	0.13358 (0.00605)	0.01343 (0.00457)	0.16505 (0.01024)	0.03745 (0.00507)
$\sigma = 1.5$	0.08478 (0.00477)	0.17174 (0.0077)	0.12695 (0.0052)	0.00632 (0.00227)	0.15309 (0.00656)	0.03194 (0.00343)
$\sigma = 2$	0.08258 (0.00462)	0.16897 (0.00656)	0.12407 (0.0055)	0.00277 (0.00113)	0.14888 (0.00641)	0.02837 (0.00307)
$\sigma = 3$	0.08263 (0.00528)	0.17131 (0.00812)	0.12526 (0.00619)	0.00148 (0.00065)	0.15241 (0.00904)	0.02726 (0.00271)
$\sigma = 4$	0.08401 (0.00712)	0.17523 (0.01094)	0.1276 (0.00841)	0.00122 (0.00061)	0.15688 (0.01171)	0.02707 (0.00269)
$\sigma = 5$	0.086 (0.00937)	0.18033 (0.01472)	0.13166 (0.0122)	0.00111 (0.00055)	0.16262 (0.01562)	0.02743 (0.00271)
$\sigma = 7$	0.09075 (0.01588)	0.19129 (0.02182)	0.13902 (0.01859)	0.00113 (0.0006)	0.17568 (0.02448)	0.02885 (0.00414)
$\sigma = 10$	0.10489 (0.04438)	0.2085 (0.03194)	0.15357 (0.03057)	0.0012 (0.00064)	0.19665 (0.03449)	0.0327 (0.00991)
$\sigma = 15$	0.13726 (0.09346)	0.23672 (0.04283)	0.1777 (0.04876)	0.00124 (0.00066)	0.22998 (0.04567)	0.0426 (0.02799)
$\sigma = 25$	0.20047 (0.14668)	0.27652 (0.05081)	0.22156 (0.08108)	0.00534 (0.03071)	0.27344 (0.05001)	0.07615 (0.08293)

Table 4: Mean and standard deviation, in parenthesis, of 100 misclassification rates, using the whole sample, for $d_{\sigma,k}(\cdot, \cdot)$ with $\sigma \in \{1.2, 1.5, 2, 3, 4, 5, 7, 10, 15, 25\}$ and the sample simplicial depth ($\sigma = 1$). Linear DD-plot classifier.

Misclassification rates		
	Bivariate normal: difference in location & scale	
	All the sample points	The sample points outside the convex hulls
$\sigma = 5$	0.12032 (0.00527)	0 (0)

Table 5: Mean and standard deviation, in parenthesis, of 100 misclassification rates, of the points outside the data convex hull and of all the sample points, for $d_{\sigma,n}(\cdot, \cdot)$ with $\sigma = 5$. Linear DD-plot classifier.

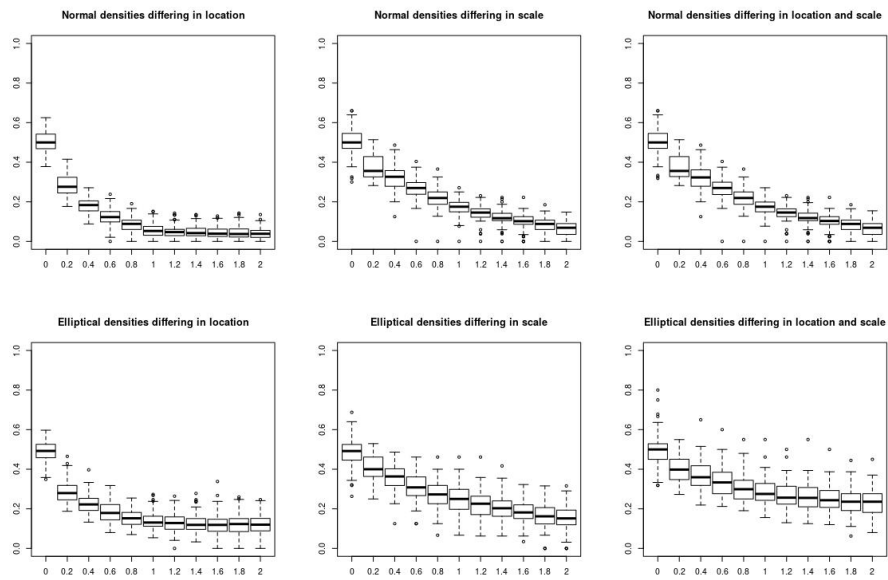


Figure 10: Boxplots of 100 misclassification rates of the points outside the data convex hull for $d_{\eta,n}(\cdot, \cdot)$ with $\eta \in \{0.2, 0.4, 0.6, 0.8, 1, 1.2, 1.4, 1.6, 1.8, 2\}$ and the sample halfspace depth ($\eta = 0$). Linear DD-plot classifier.

Misclassification rates for the points outside the convex hulls						
	Bivariate normal			Bivariate elliptical		
	location	scale	location & scale	location	scale	location & scale
halfspace	0.50610 (0.05620)	0.50221 (0.06839)	0.50376 (0.06774)	0.49016 (0.04936)	0.48796 (0.07104)	0.49512 (0.07697)
$\eta = 0.1$	0.34105 (0.05124)	0.40095 (0.06065)	0.40056 (0.06071)	0.32452 (0.04493)	0.42125 (0.06474)	0.41875 (0.07825)
$\eta = 0.2$	0.28204 (0.04775)	0.37351 (0.05931)	0.37386 (0.05891)	0.28462 (0.05144)	0.40578 (0.06147)	0.39974 (0.06861)
$\eta = 0.4$	0.18160 (0.03912)	0.32155 (0.05530)	0.32184 (0.05532)	0.22677 (0.04951)	0.36022 (0.06481)	0.36798 (0.07278)
$\eta = 0.6$	0.12216 (0.04259)	0.26719 (0.05189)	0.26678 (0.05255)	0.18378 (0.05082)	0.31097 (0.06482)	0.33542 (0.07050)
$\eta = 0.8$	0.08509 (0.03854)	0.21986 (0.04942)	0.22019 (0.04981)	0.15495 (0.04241)	0.27427 (0.06808)	0.30445 (0.06706)
$\eta = 1$	0.05591 (0.03625)	0.17478 (0.04043)	0.17527 (0.04099)	0.14143 (0.04508)	0.24846 (0.06935)	0.28583 (0.06559)
$\eta = 1.2$	0.04905 (0.03333)	0.14405 (0.03888)	0.14438 (0.03877)	0.13095 (0.04746)	0.22192 (0.06542)	0.27061 (0.06552)
$\eta = 1.4$	0.04798 (0.03073)	0.12010 (0.03649)	0.12069 (0.03694)	0.12682 (0.04703)	0.20243 (0.06136)	0.25823 (0.06860)
$\eta = 1.6$	0.04455 (0.02990)	0.09916 (0.03903)	0.09953 (0.03930)	0.12278 (0.05075)	0.18620 (0.05620)	0.24916 (0.06280)
$\eta = 1.8$	0.04462 (0.03268)	0.08197 (0.03992)	0.08228 (0.04043)	0.12315 (0.04721)	0.16605 (0.06031)	0.23744 (0.06494)
$\eta = 2$	0.04162 (0.02886)	0.06313 (0.03683)	0.06364 (0.03773)	0.12137 (0.04498)	0.15561 (0.05951)	0.23412 (0.06530)
$\eta = 2.5$	0.04161 (0.02792)	0.02541 (0.02616)	0.02634 (0.02926)	0.13799 (0.05368)	0.13279 (0.05960)	0.21951 (0.06895)
$\eta = 3$	0.04077 (0.02924)	0.00909 (0.01524)	0.01096 (0.02359)	0.17080 (0.07194)	0.11188 (0.05851)	0.20641 (0.07078)
$\eta = 3.5$	0.04178 (0.02964)	0.00319 (0.00799)	0.01210 (0.03466)	0.20742 (0.08552)	0.09536 (0.05902)	0.19391 (0.07533)
$\eta = 4$	0.04188 (0.02993)	0.00097 (0.00390)	0.02632 (0.05249)	0.23270 (0.09597)	0.08132 (0.05611)	0.18080 (0.06711)

Table 6: Mean and standard deviation, in parenthesis, of 100 misclassification rates of the points outside the data convex hull for $d_{\eta,n}(\cdot, \cdot)$ with $\eta \in \{0.1, 0.2, 0.4, 0.6, 0.8, 1, 1.2, 1.4, 1.6, 1.8, 2, 2.5, 3, 3.5, 4\}$ and the sample halfspace depth ($\eta = 0$). Linear DD-plot classifier.

Misclassification rates						
	Bivariate normal			Bivariate elliptical		
	location	scale	location & scale	location	scale	location & scale
halfspace	0.08729 (0.00445)	0.17213 (0.00748)	0.12766 (0.00553)	0.00853 (0.00259)	0.15249 (0.00714)	0.03188 (0.00315)
$\eta = 0.1$	0.08534 (0.00437)	0.17058 (0.00702)	0.12623 (0.00511)	0.00638 (0.00180)	0.14891 (0.00629)	0.03045 (0.00309)
$\eta = 0.2$	0.08414 (0.00464)	0.16935 (0.00653)	0.12588 (0.00516)	0.00524 (0.00163)	0.14828 (0.00575)	0.0298 (0.00283)
$\eta = 0.4$	0.08233 (0.00419)	0.16840 (0.00681)	0.12467 (0.00543)	0.00382 (0.00114)	0.14753 (0.00571)	0.02893 (0.00291)
$\eta = 0.6$	0.08162 (0.00419)	0.16747 (0.00620)	0.12403 (0.00514)	0.00305 (0.00093)	0.14920 (0.00603)	0.02858 (0.00279)
$\eta = 0.8$	0.08107 (0.00387)	0.16650 (0.00646)	0.12346 (0.00471)	0.00262 (0.00088)	0.15172 (0.00594)	0.02914 (0.00274)
$\eta = 1$	0.08086 (0.00416)	0.16614 (0.00597)	0.12342 (0.00517)	0.00245 (0.00089)	0.15405 (0.00578)	0.02996 (0.00291)
$\eta = 1.2$	0.08069 (0.00414)	0.16614 (0.00595)	0.12351 (0.00529)	0.00234 (0.00094)	0.15769 (0.00568)	0.03106 (0.00298)
$\eta = 1.4$	0.08076 (0.00433)	0.16580 (0.00590)	0.12361 (0.00492)	0.00227 (0.00098)	0.16127 (0.00600)	0.03247 (0.00320)
$\eta = 1.6$	0.08043 (0.00429)	0.16527 (0.00570)	0.12448 (0.00494)	0.00219 (0.00095)	0.16521 (0.00596)	0.03374 (0.00318)
$\eta = 1.8$	0.08035 (0.00418)	0.16589 (0.00585)	0.12518 (0.00513)	0.00228 (0.00091)	0.16915 (0.00585)	0.03530 (0.00342)
$\eta = 2$	0.08043 (0.00422)	0.16534 (0.00604)	0.12640 (0.00513)	0.00234 (0.00089)	0.17307 (0.00635)	0.03704 (0.00354)
$\eta = 2.5$	0.08062 (0.00420)	0.16556 (0.00618)	0.13126 (0.00552)	0.00366 (0.00124)	0.18234 (0.00712)	0.04277 (0.00446)
$\eta = 3$	0.08031 (0.00372)	0.17436 (0.00628)	0.13850 (0.00577)	0.00721 (0.00154)	0.1906 (0.00684)	0.05160 (0.00472)
$\eta = 3.5$	0.08032 (0.00405)	0.21911 (0.00600)	0.15001 (0.00539)	0.01439 (0.00235)	0.1906 (0.00684)	0.06475 (0.00557)
$\eta = 4$	0.08118 (0.00421)	0.27396 (0.00556)	0.16700 (0.00512)	0.02678 (0.00279)	0.20173 (0.00768)	0.08115 (0.00625)

Table 7: Mean and standard deviation, in parenthesis, of 100 misclassification rates, using the whole sample, for $d_{\eta,n}(\cdot, \cdot)$ with $\eta \in \{0.1, 0.2, 0.4, 0.6, 0.8, 1, 1.2, 1.4, 1.6, 1.8, 2, 2.5, 3, 3.5, 4\}$ and the sample halfspace depth ($\eta = 0$). Linear DD-plot classifier.

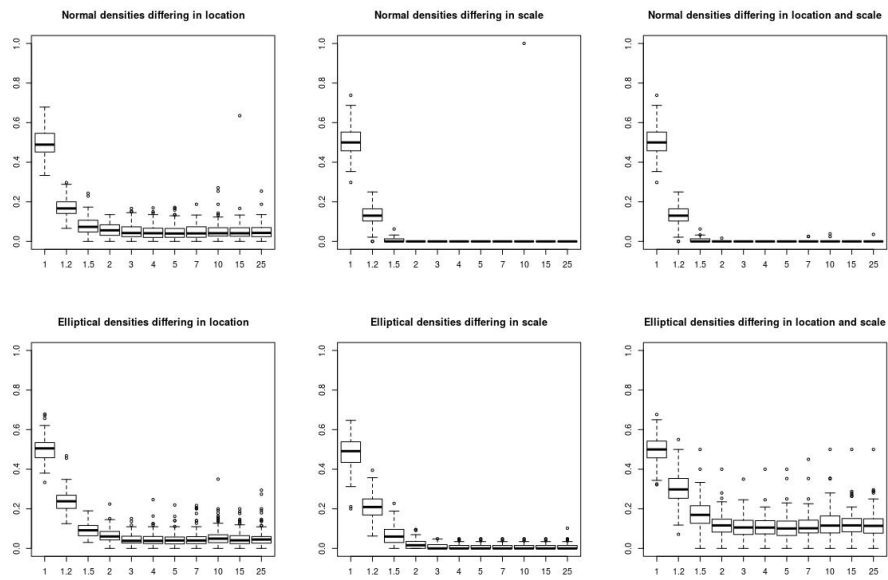


Figure 11: Boxplots of 100 misclassification rates of the points outside the data convex hull for $d_{\Delta,n}(\cdot, \cdot)$ with $\sigma \in \{1.2, 1.5, 2, 3, 4, 5, 7, 10, 15, 25\}$ and the sample simplicial depth ($\sigma = 1$). Polynomial up to degree 10 DD-plot classifier.

Misclassification rates for the points outside the convex hulls						
	Bivariate normal			Bivariate elliptical		
	location	scale	location & scale	location	scale	location & scale
$\sigma = 1$	0.49732 (0.06462)	0.50207 (0.074)	0.50207 (0.074)	0.50357 (0.06167)	0.48017 (0.08544)	0.49984 (0.07025)
$\sigma = 1.2$	0.17052 (0.0512)	0.13016 (0.04937)	0.13016 (0.04937)	0.23819 (0.05973)	0.21283 (0.06477)	0.30229 (0.08172)
$\sigma = 1.5$	0.07871 (0.04368)	0.00632 (0.01123)	0.00648 (0.0115)	0.09408 (0.0367)	0.06499 (0.04883)	0.17856 (0.07926)
$\sigma = 2$	0.05896 (0.03592)	0 (0)	0.00016 (0.00163)	0.06441 (0.03504)	0.0205 (0.02448)	0.12135 (0.05865)
$\sigma = 3$	0.05002 (0.03775)	0 (0)	0 (0)	0.04683 (0.02945)	0.00915 (0.01378)	0.11281 (0.0561)
$\sigma = 4$	0.04892 (0.03746)	0 (0)	0 (0)	0.0459 (0.03508)	0.00721 (0.012)	0.10956 (0.05638)
$\sigma = 5$	0.0485 (0.03873)	0 (0)	0 (0)	0.04552 (0.03455)	0.00665 (0.01149)	0.10907 (0.06425)
$\sigma = 7$	0.04879 (0.0368)	0 (0)	0.0005 (0.0035)	0.0513 (0.04397)	0.00652 (0.0115)	0.1141 (0.06657)
$\sigma = 10$	0.0533 (0.04677)	0.01 (0.0995)	0.00062 (0.00445)	0.05998 (0.05236)	0.00652 (0.0115)	0.12862 (0.07688)
$\sigma = 15$	0.05473 (0.06754)	0 (0)	0 (0)	0.05234 (0.03976)	0.00652 (0.0115)	0.12286 (0.06933)
$\sigma = 25$	0.05144 (0.04007)	0 (0)	0.00035 (0.00351)	0.05548 (0.05044)	0.00755 (0.01521)	0.1227 (0.07305)
$\sigma = 50$	0.05803 (0.04614)	0.00116 (0.01157)	0.00015 (0.00146)	0.04213 (0.02762)	0.00972 (0.0351)	0.13443 (0.08841)
$\sigma = 10^2$	0.05379 (0.05896)	0.00103 (0.0102)	0.00083 (0.00829)	0.03886 (0.02508)	0.01114 (0.02441)	0.16052 (0.09903)
$\sigma = 10^3$	0.04974 (0.03532)	0 (0)	0 (0)	0.03742 (0.02744)	0.00652 (0.0115)	0.21134 (0.11467)
$\sigma = 10^4$	0.04995 (0.03625)	0 (0)	0 (0)	0.11982 (0.06519)	0.00652 (0.0115)	0.20651 (0.11172)
$\sigma = 10^5$	0.04937 (0.03736)	0 (0)	0 (0)	0.13915 (0.05806)	0.00652 (0.0115)	0.20548 (0.1135)

Table 8: Mean and standard deviation, in parenthesis, of 100 misclassification rates of the points outside the data convex hull for $d_{\Delta, n}(\cdot, \cdot)$ with $\sigma \in \{1.2, 1.5, 2, 3, 4, 5, 7, 10, 15, 25, 50, 10^2, 10^3, 10^4, 10^5\}$ and the sample simplicial depth ($\sigma = 1$). Polynomial up to degree 10 DD-plot classifier.

Misclassification rates						
	Bivariate normal			Bivariate elliptical		
	location	scale	location & scale	location	scale	location & scale
$\sigma = 1$	0.08989 (0.00593)	0.17396 (0.00668)	0.12949 (0.00636)	0.01854 (0.06922)	0.15978 (0.00797)	0.03391 (0.00377)
$\sigma = 1.2$	0.08444 (0.00466)	0.16923 (0.00603)	0.12523 (0.00464)	0.02425 (0.09737)	0.15356 (0.00927)	0.03006 (0.00287)
$\sigma = 1.5$	0.08224 (0.0044)	0.16631 (0.00643)	0.1226 (0.00502)	0.00203 (0.00083)	0.1461 (0.00578)	0.02813 (0.00675)
$\sigma = 2$	0.08076 (0.00422)	0.16545 (0.00619)	0.12095 (0.0048)	0.00149 (0.00064)	0.14403 (0.00529)	0.02593 (0.00216)
$\sigma = 3$	0.08046 (0.00406)	0.16528 (0.00629)	0.12089 (0.00545)	0.00112 (0.00056)	0.14518 (0.00543)	0.02583 (0.00227)
$\sigma = 4$	0.08047 (0.0041)	0.16483 (0.00631)	0.12071 (0.00524)	0.00109 (0.00063)	0.14614 (0.00534)	0.02598 (0.00243)
$\sigma = 5$	0.08037 (0.00401)	0.16452 (0.00573)	0.12069 (0.00523)	0.00112 (0.00072)	0.14634 (0.00538)	0.02587 (0.00242)
$\sigma = 7$	0.08068 (0.00409)	0.16456 (0.00605)	0.12084 (0.00478)	0.00118 (0.0008)	0.14645 (0.00529)	0.02595 (0.00244)
$\sigma = 10$	0.08058 (0.00404)	0.16527 (0.0085)	0.12056 (0.00496)	0.00132 (0.00091)	0.14656 (0.00535)	0.02619 (0.00242)
$\sigma = 15$	0.0803 (0.0041)	0.16454 (0.0062)	0.12106 (0.00446)	0.00121 (0.00077)	0.1464 (0.0052)	0.02617 (0.00234)
$\sigma = 25$	0.08009 (0.00368)	0.16493 (0.00591)	0.12133 (0.00466)	0.00125 (0.0009)	0.14614 (0.00551)	0.02593 (0.00233)
$\sigma = 50$	0.08071 (0.00441)	0.16533 (0.00609)	0.1224 (0.00436)	0.00104 (0.00054)	0.14673 (0.00531)	0.02626 (0.00245)
$\sigma = 10^2$	0.08007 (0.00431)	0.16423 (0.00622)	0.12332 (0.00531)	0.00095 (0.00048)	0.14668 (0.00572)	0.02831 (0.00262)
$\sigma = 10^3$	0.08086 (0.00404)	0.16472 (0.00599)	0.12399 (0.00495)	0.00093 (0.00057)	0.14685 (0.00543)	0.02994 (0.00288)
$\sigma = 10^4$	0.08228 (0.00601)	0.16479 (0.00585)	0.12399 (0.00496)	0.00264 (0.00143)	0.14663 (0.00546)	0.03006 (0.00282)
$\sigma = 10^5$	0.08227 (0.00533)	0.16498 (0.00628)	0.12377 (0.00467)	0.0029 (0.00105)	0.14658 (0.00585)	0.02994 (0.00295)

Table 9: Mean and standard deviation, in parenthesis, of 100 misclassification rates, using the whole sample, for $d_{\Delta,n}(\cdot, \cdot)$ with $\sigma \in \{1.2, 1.5, 2, 3, 4, 5, 7, 10, 15, 25, 50, 10^2, 10^3, 10^4, 10^5\}$ and the sample simplicial depth ($\sigma = 1$). Polynomial up to degree 10 DD-plot classifier.

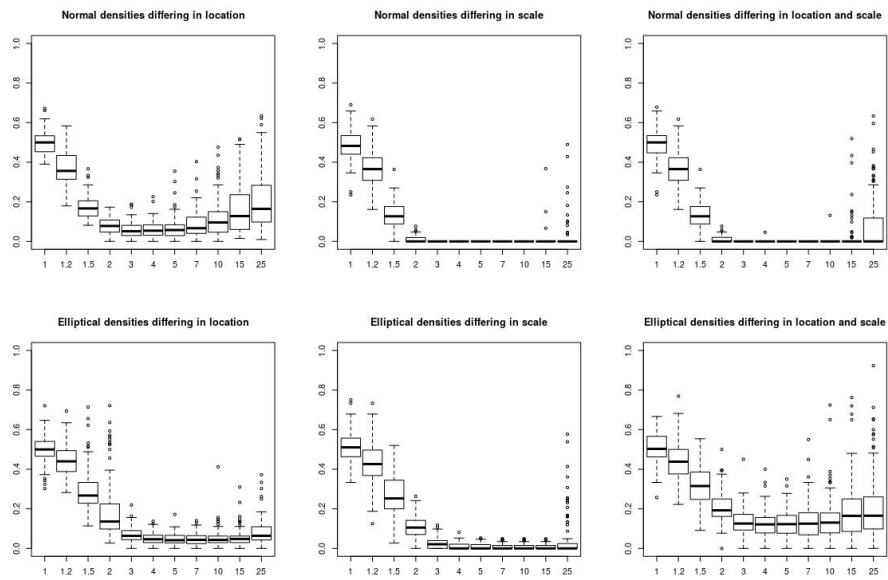


Figure 12: Boxplots of 100 misclassification rates of the points outside the data convex hull for $d_{\sigma,k}(\cdot, \cdot)$ with $\sigma \in \{1.2, 1.5, 2, 3, 4, 5, 7, 10, 15, 25\}$ and the sample simplicial depth ($\sigma = 1$). Polynomial up to degree 10 DD-plot classifier.

Misclassification rates for the points outside the convex hulls						
	Bivariate normal			Bivariate elliptical		
	location	scale	location & scale	location	scale	location & scale
$\sigma = 1$	0.49621 (0.05767)	0.4855 (0.0742)	0.48947 (0.07485)	0.49928 (0.0637)	0.50874 (0.07821)	0.50782 (0.07413)
$\sigma = 1.2$	0.36848 (0.08188)	0.36913 (0.08746)	0.36886 (0.08716)	0.44694 (0.0762)	0.42281 (0.11184)	0.44652 (0.09341)
$\sigma = 1.5$	0.17378 (0.05486)	0.13494 (0.06659)	0.1349 (0.06659)	0.29468 (0.10508)	0.26839 (0.10189)	0.32297 (0.09259)
$\sigma = 2$	0.07822 (0.04111)	0.01032 (0.01593)	0.01047 (0.01605)	0.19414 (0.14778)	0.10648 (0.05672)	0.20827 (0.07695)
$\sigma = 3$	0.05736 (0.03949)	0 (0)	0 (0)	0.0688 (0.03557)	0.02628 (0.02824)	0.13914 (0.06712)
$\sigma = 4$	0.06122 (0.04154)	0 (0)	0.00046 (0.00457)	0.05108 (0.0281)	0.01252 (0.01697)	0.12612 (0.06857)
$\sigma = 5$	0.06841 (0.05805)	0 (0)	0 (0)	0.0462 (0.02756)	0.00931 (0.01381)	0.12683 (0.06851)
$\sigma = 7$	0.08625 (0.06802)	0 (0)	0 (0)	0.04603 (0.02818)	0.00702 (0.01196)	0.13925 (0.09446)
$\sigma = 10$	0.11768 (0.09665)	0 (0)	0.00132 (0.01309)	0.05072 (0.04722)	0.00686 (0.01195)	0.15373 (0.11603)
$\sigma = 15$	0.16861 (0.13244)	0.00584 (0.03984)	0.02418 (0.08402)	0.05538 (0.04437)	0.00686 (0.01181)	0.18643 (0.14561)
$\sigma = 25$	0.20819 (0.15409)	0.02198 (0.07715)	0.0872 (0.14601)	0.08309 (0.06538)	0.05069 (0.11057)	0.21467 (0.17448)

Table 10: Mean and standard deviation, in parenthesis, of 100 misclassification rates of the points outside the data convex hull for $d_{\sigma,k}(\cdot, \cdot)$ with $\sigma \in \{1.2, 1.5, 2, 3, 4, 5, 7, 10, 15, 25\}$ and the sample simplicial depth ($\sigma = 1$). Polynomial up to degree 10 DD-plot classifier.

Misclassification rates						
	Bivariate normal			Bivariate elliptical		
	location	scale	location & scale	location	scale	location & scale
$\sigma = 1$	0.10896 (0.05565)	0.19224 (0.0107)	0.14491 (0.00892)	0.04843 (0.1066)	0.18008 (0.01439)	0.04524 (0.00716)
$\sigma = 1.2$	0.09162 (0.00559)	0.17909 (0.00788)	0.13334 (0.00634)	0.05285 (0.13329)	0.16211 (0.00935)	0.03659 (0.00466)
$\sigma = 1.5$	0.08496 (0.00446)	0.17129 (0.0081)	0.12698 (0.00582)	0.0607 (0.15505)	0.15287 (0.00757)	0.03123 (0.00311)
$\sigma = 2$	0.08201 (0.00462)	0.16861 (0.0069)	0.12336 (0.00516)	0.07262 (0.17244)	0.14884 (0.00636)	0.02814 (0.00295)
$\sigma = 3$	0.08247 (0.00515)	0.17014 (0.00701)	0.12415 (0.00598)	0.00145 (0.00058)	0.15089 (0.00744)	0.0269 (0.0025)
$\sigma = 4$	0.08354 (0.00672)	0.17205 (0.00853)	0.12651 (0.00786)	0.00117 (0.00053)	0.154 (0.00906)	0.02676 (0.00259)
$\sigma = 5$	0.08506 (0.00907)	0.17471 (0.01089)	0.12937 (0.0113)	0.00108 (0.00052)	0.15782 (0.01278)	0.02715 (0.00253)
$\sigma = 7$	0.08985 (0.01556)	0.18306 (0.0168)	0.13682 (0.01761)	0.00107 (0.00046)	0.16661 (0.01847)	0.02926 (0.00439)
$\sigma = 10$	0.10132 (0.0361)	0.19618 (0.02443)	0.1474 (0.02788)	0.00108 (0.00058)	0.18179 (0.02632)	0.03507 (0.01006)
$\sigma = 15$	0.11862 (0.05746)	0.21818 (0.03543)	0.16244 (0.03606)	0.0012 (0.00077)	0.20708 (0.03645)	0.04424 (0.02118)
$\sigma = 25$	0.13417 (0.06822)	0.25058 (0.04147)	0.18426 (0.04462)	0.00368 (0.01614)	0.23961 (0.04249)	0.05402 (0.03443)

Table 11: Mean and standard deviation, in parenthesis, of 100 misclassification rates, using the whole sample, for $d_{\sigma,k}(\cdot, \cdot)$ with $\sigma \in \{1.2, 1.5, 2, 3, 4, 5, 7, 10, 15, 25\}$ and the sample simplicial depth ($\sigma = 1$). Polynomial up to degree 10 DD-plot classifier.

References

- Miguel A. Arcones and Evarist Giné. Limit theorems for u-processes. *The Annals of Probability*, 21(3):1494–1542, 1993.
- Miguel A. Arcones, Chen Zhiqiang, and Evarist Giné. Estimators related to u-processes with applications to multivariate medians: asymptotic normality. *The Annals of Statistics*, 22(3):1460–1477, 1994.
- Michael Burr and Robert Fabrizio. Error probabilities for halfspace depth. *arXiv preprint arXiv:1605.04323*, 2016.
- Juan A. Cuesta-Albertos, Manuel Febrero-Bande, and M Oviedo de la Fuente. The dd^g -classifier in the functional setting. *Test*, 26(1):119–142, 2017.
- John HJ Einmahl, Jun Li, and Regina Y Liu. Bridging centrality and extremity: Refining empirical data depth using extreme value statistics. *The Annals of Statistics*, 43(6):2738–2765, 2015.
- Otto JWF Kardaun. *Classical methods of statistics: with applications in fusion-oriented plasma physics*. Springer Science & Business Media, 2005.
- Vladimir S Korolyuk and Yu V Borovskich. *Theory of U-statistics*, volume 273. Springer Science & Business Media, 2013.
- Christophe Ley and Davy Paindaveine. Depth-based runs tests for multivariate central symmetry. *ECORE Discussion Papers*, 22, 2011.
- Jun Li, Juan A. Cuesta-Albertos, and Regina Y. Liu. Dd-classifier: Nonparametric classification procedure based on dd-plot. *Journal of the American Statistical Association*, 107(498):737–753, 2012. ISSN 01621459.
- R. Y. Liu. On a notion of data depth based on random simplices. *The Annals of Statistics*, 18(1):405–414, 1990.
- Jean-Claude Massé. Asymptotics for the tukey median. *Journal of Multivariate Analysis*, 81(2):286–300, 2002.
- Jean-Claude Massé. Asymptotics for the tukey depth process, with an application to a multivariate trimmed mean. *Bernoulli*, 10(3):397–419, 2004.
- Stanislav Nagy and Jiří Dvořák. Illumination depth. *arXiv e-prints*, art. arXiv:1905.04119, 2019.
- Oleksii Pokotylo, Pavlo Mozharovskyi, and Rainer Dyckerhoff. Depth and depth-based classification with r-package ddalpha. *arXiv:1608.04109*, 2016.
- Peter J Rousseeuw and Ida Ruts. The depth function of a population distribution. *Metrika*, 49:213–244, 1999.
- Robert J Serfling. Multivariate symmetry and asymmetry. *Encyclopedia of statistical sciences*, 8, 2004.

- John W. Tukey. Mathematics and the picturing of data. In *Proceedings of the International Congress of Mathematicians (Vancouver, B. C., 1974)*, Vol. 2, pages 523–531. Canad. Math. Congress, Montreal, Que., 1975.
- Yijun Zuo and Robert Serfling. General notions of statistical depth function. *Annals of statistics*, pages 461–482, 2000a.
- Yijun Zuo and Robert Serfling. On the performance of some robust nonparametric location measures relative to a general notion of multivariate symmetry. *Journal of Statistical Planning and Inference*, 84(1-2):55–79, 2000b.
- Yijun Zuo and Robert Serfling. Structural properties and convergence results for contours of sample statistical depth functions. *Ann. Statist.*, 28(2):483–499, 04 2000c. doi: 10.1214/aos/1016218227. URL <https://doi.org/10.1214/aos/1016218227>.